AD_____

Award Number: W81XWH-07-1-0150

TITLE: Role of MAPK activation in Prostate Cancer Development and Progression

PRINCIPAL INVESTIGATOR: Hyeong-nam Jeong

CONTRACTING ORGANIZATION: Dana-Farber Cancer Institute
Boston, MA 02115

REPORT DATE: March 2008

TYPE OF REPORT: Annual Summary

PREPARED FOR: U.S. Army Medical Research and Materiel Command
Fort Detrick, Maryland 21702-5012

# REPORT DOCUMENTATION PAGE

*Form Approved*
*OMB No. 0704-0188*



| **1. REPORT DATE** *(DD-MM-YYYY)* | **2. REPORT TYPE** | **3. DATES COVERED** *(From - To)* |
|---|---|---|
| 01-03-2008 | Annual Summary | 15 FEB 2007 - 14 FEB 2008 |

**4. TITLE AND SUBTITLE**
Role of MAPK activation in Prostate Cancer Development and Progression

**5a. CONTRACT NUMBER**

**5b. GRANT NUMBER**
W81XWH-07-1-0150

**5c. PROGRAM ELEMENT NUMBER**

**6. AUTHOR(S)**
Hyeong-nam Jeong

E-Mail: hyeong-nam_jeong@dfci.harvard.edu

**5d. PROJECT NUMBER**

**5e. TASK NUMBER**

**5f. WORK UNIT NUMBER**

**7. PERFORMING ORGANIZATION NAME(S) AND ADDRESS(ES)**

Dana-Farber Cancer Institute
Boston, MA 02115

**8. PERFORMING ORGANIZATION REPORT NUMBER**

**9. SPONSORING / MONITORING AGENCY NAME(S) AND ADDRESS(ES)**
U.S. Army Medical Research and Materiel Command
Fort Detrick, Maryland 21702-5012

**10. SPONSOR/MONITOR'S ACRONYM(S)**

**11. SPONSOR/MONITOR'S REPORT NUMBER(S)**

**12. DISTRIBUTION / AVAILABILITY STATEMENT**
Approved for Public Release; Distribution Unlimited

**13. SUPPLEMENTARY NOTES**

**14. ABSTRACT**

Although Prostate cancer is the most common and second leading cause of cancer-related deaths in American men, lack of animal models that faithfully recapitulate histopathological and clinical features of human prostate cancer has hampered prostate cancer research. Taking advantage of a unique androgen-insensitive transgene promoter system, we developed a novel genetically-engineered mouse (GEM) model of invasive prostate adenocarcinoma whereby an activating mutation of BRAFV600E has been targeted to the epithelial compartment of the prostate gland. As a first step for the characterization of this model, we attempted to assess the requirement for continuous BRAF*-ERK activation in maintenance of established invasive lesions and in progression to androgen-independent state. To our surprise, we found that while sufficient to initiate development of AKT-independent invasive prostate adenocarcinoma, BRAFV600E is not required for its maintenance. In addition, we also demonstrated that BRAF driven ERK and S6K activation alone is not sufficient to drive androgen-independent growth post castration in this mouse model, although it appears to be permissive of survival in low androgen state.

**15. SUBJECT TERMS**
No subject term provided.

| **16. SECURITY CLASSIFICATION OF:** | | | **17. LIMITATION OF ABSTRACT** | **18. NUMBER OF PAGES** | **19a. NAME OF RESPONSIBLE PERSON** |
|---|---|---|---|---|---|
| **a. REPORT** | **b. ABSTRACT** | **c. THIS PAGE** | | | USAMRMC |
| U | U | U | UU | 42 | **19b. TELEPHONE NUMBER** *(include area code)* |

## Table of Contents

**Page**

## Introduction

Prostate cancer is the second leading cause of cancer-related deaths in men. Activation of MAP kinase signaling pathway has been implicated in advanced and androgen-independent prostate cancers, although formal genetic proof has been lacking. Taking advantage of a unique androgen-insensitive transgene promoter system, we developed a novel genetically-engineered mouse (GEM) model of invasive prostate adenocarcinoma whereby an activating mutation of $BRAF^{V600E}$ – a mutation found in ~10% of human prostate tumors – has been targeted to the epithelial compartment of the prostate gland. These GEM mice developed prostate gland hyperplasia with progression to rapidly growing AKT-independent invasive adenocarcinoma, providing genetic proof that activation of MAP kinase signaling alone without concurrent AKT-activation is sufficient to drive prostate tumorigenesis. Based on these preliminary data, we proposed two specific aims for DoD prostate cancer training award: 1) *To characterize the Sca-1+ cells in iBRAF* prostate epithelium and tumor.* 2) *To assess the requirement for continuous BRAF*-ERK activation in maintenance of established invasive lesions and in progression to androgen-independent state.* We attempted to address the second specific aim first. First, to address a proposed question "Does iBRAF*-driven tumor regress after doxycycline withdrawal?", we performed doxycycline withdrawal study in tumor-bearing iBRAF* transgenic animals, and the changes of tumor volume was monitored by serial MRI imaging. In addition, we used pharmacological inhibition of MEK with CI-1040 in renal capsule grafts of iBRAF* tumors (n=2). Unexpectedly, tumors continued to grow in both systems, indicating that genetic extinction of $BRAF^{V600E}$ in established prostate tumors did not lead to tumor regression. Therefore, while sufficient to initiate development of AKT-independent invasive prostate adenocarcinoma, $BRAF^{V600E}$ is not required for its maintenance. Second, to address a proposed question "Does iBRAF*-driven tumor regress after castration?", we performed castration study in tumor-bearing iBRAF* transgenic animals and renal capsule grafts. Histopathological examination identified residual tumor nodules in two systems after castration, but they didn't grow, suggesting that BRAF driven ERK and S6K activation alone is not sufficient to drive androgen-independent growth post castration, although it appears to be permissive of survival in low androgen state.

## Results

### *A) Proposed research plan.*

**Specific Aim #2. To assess the requirement for continuous BRAF*-ERK activation in maintenance of established invasive lesions and in progression to androgen-independent state.**

In human, prostate cancer invariably recur after androgen ablation in an androgen independent form [2]. While our data in the iBRAF* model has shown that ERK activation can drive prostate tumor development, the goal of this aim is to determine whether BRAF*-ERK activation is required for maintenance and progression of prostate tumors. Specifically, I will address whether iBRAF*-driven prostate tumor regress upon doxycycline-withdrawal (extinction of BRAF* expression) or androgen ablation.

***Does iBRAF*-driven tumor regress after doxycycline withdrawal?*** Here, I will determine the requirement for continuous BRAF*-ERK activation in maintenance of established invasive prostate tumors. Upon documentation of baseline tumors by MRI, 40 tumor-bearing iBRAF* male mice will be randomized to doxycycline withdrawal (experimental) or doxycycline administration (control) cohorts (n=20 each). Tumor volumes will be monitored by serial MRI imaging every week (cf. Preliminary Results, in collaboration with Dr. Ralph Weissleder). Serial study: At 72 hours, 1 week, 2 weeks, 3 weeks, and 4 weeks after doxycycline withdrawal, two tumor-bearing mice from each cohort will be sacrificed for histological and molecular analyses (see below). Endpoint study: Remaining 10 mice from each cohort will be following for endpoint characterization. In particular, we are interested in determining the degree of regression (e.g. is regression

100%?) and duration of regression (e.g. do we see emergence of escapers? If so, in what time frame). We will consider an endpoint is reached when a tumor recurs in the absence of doxycycline, or that an animal remains tumor-free (by MRI) for a period of 6 months. At these endpoints, animals will be sacrificed and prostate and other major organs will be harvested for detailed histopathological and molecular characterization. Kanplan Meier curves will be generated to determine overall survival or disease-free survival of the ON doxycycline control and OFF-doxycycline experimental cohorts. Additional mice will be added to this study if necessary. Histopathological characterization: Tumor specimens, prostate glands and all other major organs will be harvested for fixation and section for H&E for tumor morphology, as well as IHC on panels of relevant markers (cf. Figure 5) in addition proliferation and apoptosis indices by BrdU or Ki67 and TUNEL staining. Stoma compartment will be characterized as well, with particular emphasis on tumor angiogenesis by CD31 IHC. Molecular analyses: extinction of transgene expression by doxycycline withdrawal will be documented in experimental cohort by RT-qPCR or ISH. Inactivation of ERK signaling pathway will be assessed by Western blotting. Beyond the scope of this proposal, genomic characterization of the tumors, especially the escapers, will be of particular interest.

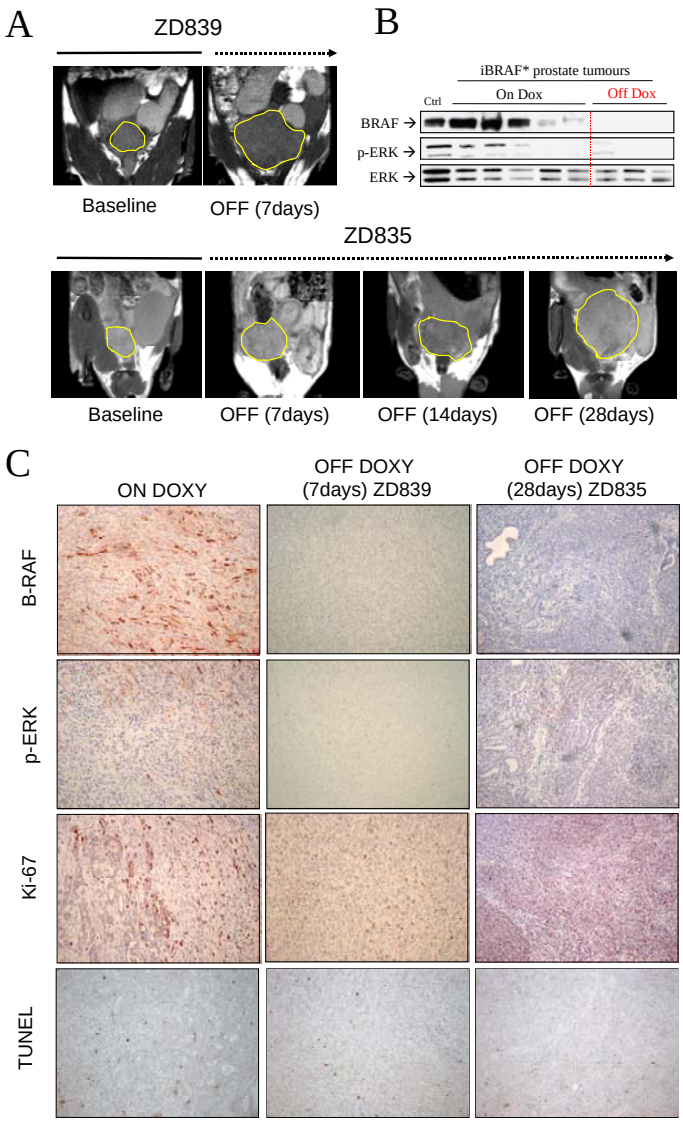


**Fig. 1.** iBRAF* prostate tumors do not require BRAF activation for their tumor maintenance. (*A*) Tumor size change was monitored by serial MRI imaging before (baseline; solid line) and after (indicated periods; dotted line) doxycycline withdrawal (7 days for ZD839 and 28 days for ZD835). Yellow line indicates tumor boundary. (*B*) B-RAF expression and p-ERK activation were not detected by immunoblotting analysis in most of off doxycycline iBRAF* PCA tumors (n=3), although one of the off doxycycline iBRAF* tumor samples (ZD835) showed weak p-ERK activation. (*C*) Immunohistological examination using antibodies against B-RAF and p-ERK confirmed the repression of B-RAF* transgene repression during off doxycycline periods (7 days for ZD839 and 28 days for ZD835). However, the tumors were viable and still growing, as manifested by low apoptosis on TUNEL and active proliferation by Ki67 staining.

***Does iBRAF*-driven tumor regress after castration?*** Here, we will perform a similar study as above, except that tumor-bearing mice will be subjected to castration, rather than doxycycline withdrawal. Our preliminary result on one mouse suggested that regression may not be observed, at least not with the same kinetics as described for other prostate tumor models. Therefore, it would be interesting to analyze the genomic and genetic characteristics of the androgen-insensitive tumors and to generate hypotheses of underlying mechanisms of development of androgen independence.

***Anticipated Results:*** If iBRAF* plays a tumor maintenance role, then doxycycline withdrawal will lead to tumor regression. It is possible that other genetic events, such as endogenous RAS activation, may substitute for transgenic BRAF*. In such case, only partial regression would be expected. On the other hand, it is possible that BRAF* is a potent activator of ERK signaling, but once activated, ERK signaling can be maintained by other regulatory feedback loop, obviating the need for continuous BRAF*. In such case, doxycycline withdrawal would have little effect on tumor regression. With respect to castration, if MAPK activation confers androgen insensitivity, then BRAF* driven tumors may demonstrate less dependence on androgen, as suggested by our preliminary data on one tumor-bearing mouse. Alternatively, it is

possible that MAPK activation is a correlative finding with emergence of androgen independence, in such case, persistent MAPK activation via BRAF* would not confer enhanced resistance to hormonal ablation.

***Future Plan.*** Beyond the scope of this training proposal, genome-wide genomic studies of tumors from these two studies will be highly informative. Here, I will be able to take advantage of the infrastructure and expertise of my mentor Dr. Chin's laboratory on array-CGH, expression profiling and bioinforomatics. Of particular relevant, a genomic study of escapers in an inducible RAS model of melanoma has led to the identification of a novel melanoma metastasis gene (Kim et al, submitted).

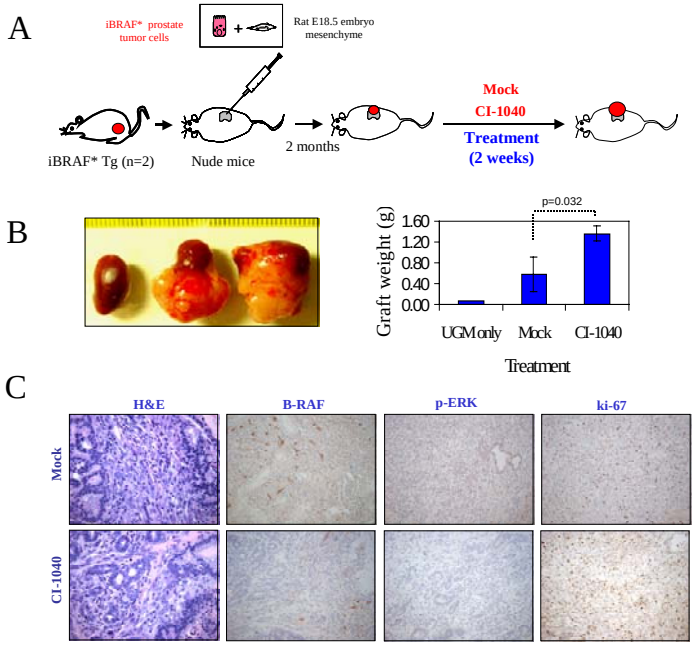


**Fig. 2.** Activation of B-RAF pathway is not required for tumor progression and maintenance. (*A*) Schematic representation of CI-1040 (a MEK inhibitor) treatment protocol using tissue recombination. Tissue recombinants were generated with iBRAF* prostate cancer cells and rat mesenchymal cells, implanted under the kidney capsule of nude mice, and grown for 2 months. The mice were orally treated with CI-1040 at 150mg/kg body weight twice a day for two weeks. (*B*) Gross morphology and graft weight after two-week treatment showed significantly increased graft size with CI-1040 treatment, compared to mock-treated control. (*C*) Histological analyses of grafts from mock-treated and CI-1040-treated mice confirmed prostate tumor development. Although decreased p-ERK staining with CI-1040-treated mice indicated the inhibition of B-RAF pathway, tumors were still proliferating, as manifested by strong positivity with Ki67 staining

***B) Accomplishment***

***a) Does iBRAF*-driven tumor regress after doxycycline withdrawal?***

To determine whether constitutive BRAF* signaling is required for iBRAF* tumor maintenance, we performed doxycycline withdrawal study in iBRAF* transgenic animals with documented PCA by MRI or by physical examination. First, two iBRAF* mice were identified as tumor-bearing and enlisted into serial MRI after doxycycline was removed from the drinking water. Unexpectedly, tumors continued to grow in both animals as shown on MRI (Fig. 1*A*), requiring termination and sacrifice of ZD839 at one week and ZD835 at 4 weeks post doxycycline withdrawal. Similarly, two additional iBRAF* mice with tumors by palpation were taken off doxycycline; close follow-up revealed continued tumor growth, requiring sacrifice at 2 weeks and 4 weeks, respectively (data not shown). These off-doxycycline tumors did not express BRAF* by Western blot analysis (Fig. 1*B*) or by IHC (Fig. 1*C*, compare immunoreactivity to left panel). Accordingly, ERK phosphorylation was undetectable in ZD839 and only patchy in ZD835. Consistent with its continued growth *in vivo*, robust Ki67 and minimal TUNEL staining was documented in these off-doxycycline tumors, similar to the profile of on-doxycycline iBRAF* PCA. Corroborating with this was the finding that pharmacological inhibition of MEK with CI-1040 in renal capsule grafts of iBRAF* tumors (n=2) did not inhibit tumor growth despite extinction of pERK activities (Fig. 2). Taken together, these observations indicate that, while sustained BRAF* activation in the prostate gland is sufficient to drive development of AKT-independent invasive prostate adenocarcinoma, it is not required for maintenance of established PCA.

***b) Does iBRAF*-driven tumor regress after castration?***

Emergence of androgen-independence represents the most significant disease process in human PCA from the standpoint of mortality, prompting us to determine whether the iBRAF* model develops androgen independent (AI) tumors. To this end, we identified 10 iBRAF* mice with documented PCA by MRI screening for heterogeneous mass in the prostate gland (representing PCA) for castration. Despite frequent bladder

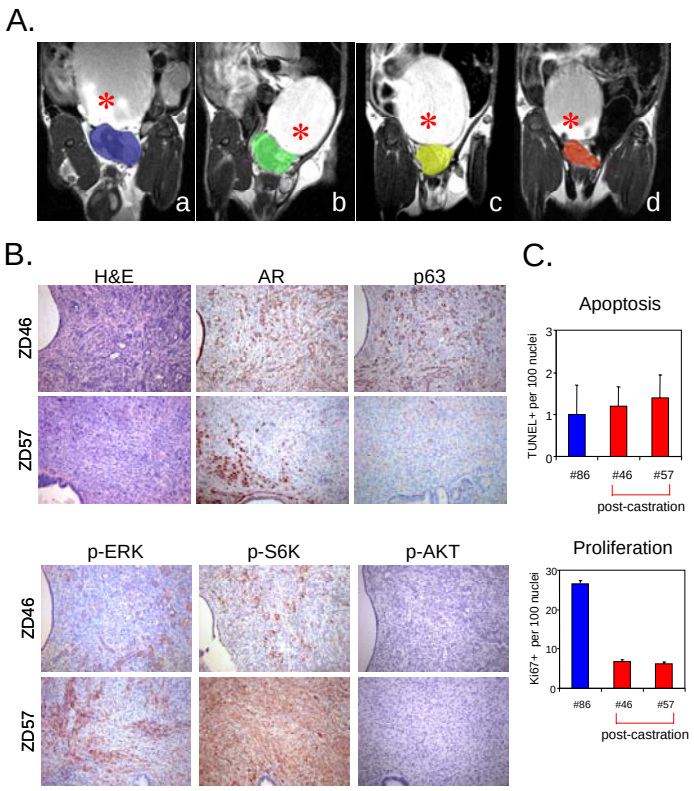


**Fig. 3.** iBRAF* PCA progress to indolent androgen-independence after castration. (*A*) The reduction of tumor volumes was monitored by MRI over a 4-week time course after castration (**a**, tumor (blue) 1 week after castration; **b**, tumor (green) 2 weeks after castration; **c**, tumor (yellow) 3 weeks after castration; **d**, tumor (orange) 4 weeks after castration). Asterisk indicates bladder. (*B*) Histological examination confirmed the presence of prostatic tumor cells in two castrated iBRAF* mice (#46 and #57). The two post-castration tumors were positive for AR (a prostatic luminal cell marker) and p63 (a basal cell marker) by IHC. Also, the post-castration tumor cells were negative for p-AKT, but remained strongly positive for p-ERK and p-S6K on IHC. (*C*) The post-castration tumor cells were viable and growing, not residual tumor remnants, as manifested by low apoptosis index (1.2 (+/-0.45) and 1.4 (+/-0.55) per 100 nuclei for #46 and #57, respectively) on TUNEL, comparable to pre-castration tumor (1.0 (+/-0.71)) (top), and active proliferation by Ki67 staining, albeit at rate much lower than that of pre-castration tumor (6.8 (+/-3.6) and 6.2 (+/-2.2) for #46 and #57, respectively and 26.6 (+/-3.6) in the pre-castrated tumors) (bottom).

irrigation in an effort to relieve outlet obstruction, 50% (n=5) animals succumbed peri-operatively which was likely due to a generally compromised physiological state secondary to renal failure. Of the surviving animals, two were sacrificed at one-week post-castration (#36 and #57) and the remaining 3 were followed by weekly MRI for 4 weeks. Volumes of the prostate mass in all 5 mice decreased during the observation period (Fig. 3*A*) but histopathological examination identified residual tumor nodules in two of the five castrated iBRAF* mice (#46 and #57). These tumor nodules were AR+ and p63+ with strong p-ERK and p-S6K activation but without detectable p-AKT (Fig. 3*B*). That they were comprised of viable malignant cells was shown by low apoptosis indice, comparable with index observed in pre-castrated tumor (Fig. 3*C*). However, compared to the rapidly growing pre-castration tumors, these post-castrated tumors were indolent, with proliferation indices of 6.8 (+/-3.6) and 6.2 (+/-2.2), respectively, compared to an index of 26.6 (+/-3.6) in the pre-castrated tumors (n= 300 nuclei/area x 5 areas counted in each sample; $p < 0.001$ for both; Fig. 3*C*). Thus, it appears that BRAF driven ERK and S6K activation alone is not sufficient to drive androgen-independent growth post castration, although it appears to be permissive of survival in low androgen state.

Alternatively, using tissue recombination system, we investigated whether constitutive BRAF* signaling is required for the emergence of androgen-independent tumor. Tissue recombinants composed of 14-week-old iBRAF* prostatic cells and UGM were implanted under kidney capsules of nude mice. Previous time-course histological analyses of iBRAF* mice demonstrated the presence of hyperplastic lesions in the prostate at the age of 14 weeks. After two months of the implantation, initial graft size before castration was measured by MRI imaging, and castration surgery was performed. Graft size change after castration was monitored by serial MRI imaging (Fig. 4*A*). Consistent with the castration study with tumor-bearing iBRAF* transgenic mice, graft size also decreased after castration in tissue recombination system (Fig. 4*B*). But, histopathological examination also identified residual ductal structures 6 weeks after castration in tissue recombination system, although most of luminal cells went apoptotic cell death. In contrast, grafts without castration showed well-developed prostatic ducual structures with hyperplastic lesions (Fig. 4*C*). Interestingly, most of the cells in residual ducts after castration showed p63+, but very weak positive for AR and p-AKT.

## *C) Discussion*

### *a) Does iBRAF*-driven tumor regress after doxycycline withdrawal?*

While MAPK activation alone can initiate prostate tumorigenesis, continued mutant BRAF expression or downstream MAPK activation is not required for maintenance of established PCA. Genetic inactivation of BRAF* by doxycycline withdrawal in 4 BRAF*-driven tumors did not lead to tumor growth inhibition nor regression. Pharmacological inhibition of MEK similarly failed to inhibit growth of renal capsule tumor grafts. Taken together, these observations indicate that continued expression of mutant BRAF or activation of MAPK is not required to sustain growth or maintain viability of established PCA. This contrasts with findings in BRAF*-driven lung adenocarcinoma model where BRAF* acts not only as an initiating oncogene but shown to be required for maintenance, highlighting the context/lineage specific role(s) of an oncogenic event in genesis, progression and maintenance.

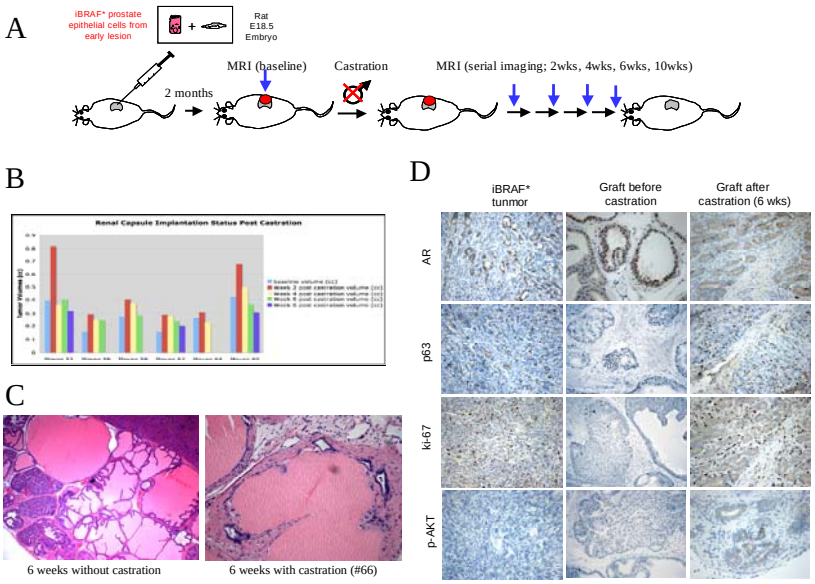


**Fig. 4.** **(A)** Cartoon for experimental design for tissue recombination, castration, and serial MRI imaging. **(B)** Graft size change after castration monitored by MRI at the indicated time. **(C)** Histology after 6 weeks after castration in comparison to histology without castration. Without castration, graft shows well developed from normal to hyperplastic prostatic ductal structure, but 6 weeks after castration, most of luminal cells are dead with some residual ductal structures. (D)Immunohistochemical analyses showed p63+ cells 6 weeks after castration, along with very weak staining of AR and p-AKT.

At first, with our assumption that iBRAF* plays a tumor maintenance role, we expected that doxycycline withdrawal would lead to tumor regression. But, to our surprise, the results we found are totally opposite. It is possible that other genetic events, such as endogenous RAS activation, may substitute for transgenic BRAF*. In such case, only partial regression would be expected. However, the tumor size with the treatment of a MEK inhibitor significantly increased compared to vehicle treated ones in tissue recombination study. On the other hand, it is possible that BRAF* is a potent activator of ERK signaling, but once activated, ERK signaling can be maintained by other regulatory feedback loop, obviating the need for continuous BRAF*. In such case, doxycycline withdrawal would have little effect on tumor regression.

### *b) Does iBRAF*-driven tumor regress after castration?*

These data suggested two possibilities. First, androgen-independent p63 basal cells survived after castration, in contrast androgen-sensitive AR+ luminal cells went apoptotic cell death. Second, after castration, unidentified androgen-independent progenitor/stem cells survived and started to differentiate into p63+ cells in this model. At this point, the possibility of further differentiation of the p63+ cells into the AR+ luminal cells under the low level of androgen needs to be investigated.

The ability to enforce MAPK activation via mutant BRAF expression under an androgen-insensitive promoter renders this iBRAF* model an ideal system for genetic dissection of MAPK contribution independent of AKT during AI progression. While they grow rapidly in androgen-rich conditions, these AKT-negative iBRAF* PCA undergo complete or significant regression upon castration. Those indolent lesions surviving castration remain pAKT negative, pointing to its dispensability for survival in low-androgen state but requirement for AI growth in vivo, in line with recent study in ex-vivo manipulated system. Thus, we conclude that while it may be permissive for survival post castration, BRAF driven MAPK activation is not sufficient to drive active AI growth under an androgen-limited state.

## Key Research Accomplishments

1. ***Constitutive activation of BRAF/ERK/MEK signaling is NOT required for iBRAF* tumor maintenance.***

   While MAPK activation alone can initiate prostate tumorigenesis, continued mutant BRAF expression or downstream MAPK activation is not required for maintenance of established PCA in iBRAF* model.

2. ***Constitutive activation of BRAF/ERK/MEK signaling is NOT sufficient to drive active AI growth under an androgen-limited state.***

   While MAPK activation may be permissive for survival post castration, BRAF driven MAPK activation is not sufficient to drive active AI growth under an androgen-limited state.

## Reportable Outcomes

1. This work was presented at The National Cancer Institute-Mouse Models of Human Cancers Consortium (MMHCC) in Washington D.C. 2008.

**Authors:** *Joseph H. Jeong, Zhenxiong Wang, Alexander R. Guimaraes, Xuesong Ouyang, Jose L. Figueiredo, Zhihu Ding, Jiang Shen, Isil Guney, Gyeong Hoon Kang, Eyoung Shin, William C. Hahn, Massimo F. Loda, Cory Abate-Shen, Ralph Weissleder, Lynda Chin,*

**Title:** Mutant BRAF activation plays causal but not maintenance role in AKT-independent invasive prostate adenocarcinoma

**Abstract:** Prostate cancer is the second leading cause of cancer-related deaths in men. Although initially effective, hormonal ablation therapy is not curative and invariably leads to emergence of androgen-independent disease which does not respond to existing therapeutics. Activation of MAP kinase signaling pathway has been implicated in advanced and androgen-independent prostate cancers, although formal genetic proof has been lacking. Taking advantage of a unique androgen-insensitive transgene promoter system, we developed a novel genetically-engineered mouse (GEM) model of invasive prostate adenocarcinoma whereby an activating mutation of $BRAF^{V600E}$ – a mutation found in ~10% of human prostate tumors – has been targeted to the basal progenitor compartment of the prostate gland. These GEM mice developed prostate gland hyperplasia with progression to AKT-independent invasive adenocarcinoma that readily transitions to androgen-independent state upon castration, thus providing unequivocal genetic proof that activation of MAP kinase signaling alone without concurrent AKT-activation is sufficient to drive prostate tumorigenesis and progression to androgen independence.

2. This work was submitted to “PNAS” for publication and currently under revision.

# Mutant BRAF activation plays causal but not maintenance role in AKT-independent invasive prostate adenocarcinoma

Joseph H. Jeong[1*], Zhenxiong Wang[1*], Alexander S. Guimaraes[2]; Xuesong Ouyang[3]; Jose L. Figueiredo[2]; Zhihu Ding[1]; Jiang Shen[1]; Isil Guney[1,8]; Gyeong Hoon Kang[4]; Eyoung Shin[5]; William C. Hahn[1,6,8]; Massimo F. Loda[1,5,8]; Cory Abate-Shen[3]; Ralph Weissleder[2]; Lynda Chin[1,7,#]

[1] Department of Medical Oncology, Dana-Farber Cancer Institute, Boston, MA
[2] Center for Molecular Imaging Research, Massachusetts General Hospital, Harvard Medical School, Charlestown, MA;
[3] Center for Advanced Biotechnology and Medicine, The Cancer Institute of New Jersey and Departments of Medicine, UMDNJ-Robert Wood Johnson Medical School, Piscataway, NJ
[4] Department of Pathology, Seoul National University College of Medicine, Seoul Korea
[5] Department of Pathology, Brigham and Women's Hospital, Harvard Medical School, Boston, MA
[6] Center for Cancer Genome Discovery, Dana-Farber Cancer Institute, Boston, MA
[7] Department of Dermatology, Harvard Medical School, Boston, MA
[8] Broad Institute of Harvard and MIT, Cambridge, MA 02142

* These authors contributed equally

# Correspondence should be addressed to LC: lynda_chin@dfci.harvard.edu

**Abstract**

Prostate cancer is the second leading cause of cancer-related deaths in men. Activation of MAP kinase signaling pathway has been implicated in advanced and androgen-independent prostate cancers, although formal genetic proof has been lacking. Taking advantage of a unique androgen-insensitive transgene promoter system, we developed a novel genetically-engineered mouse (GEM) model of invasive prostate adenocarcinoma whereby an activating mutation of $BRAF^{V600E}$ – a mutation found in ~10% of human prostate tumors – has been targeted to the epithelial compartment of the prostate gland. These GEM mice developed prostate gland hyperplasia with progression to rapidly growing AKT-independent invasive adenocarcinoma, providing genetic proof that activation of MAP kinase signaling alone without concurrent AKT-activation is sufficient to drive prostate tumorigenesis. Importantly, genetic extinction of $BRAF^{V600E}$ in established prostate tumors did not lead to tumor regression, indicating that while sufficient to initiate development of AKT-independent invasive prostate adenocarcinoma $BRAF^{V600E}$ is not required for its maintenance.

**Introduction**

Prostate cancer (PCA) is the most common malignancy affecting men over age of 65. Initially responsive to hormonal ablation therapy, PCA invariably recur and evolve to become lethal androgen-independent (AI) disease. While a number of common genetic events have been implicated in human prostate carcinogenesis including those targeting *PTEN*, *RB*, and *p27* tumor suppressors, *NKX3.1* tumor modulator, and the *c-Myc* oncogene (1-5), the genetic and biological basis governing progression to advanced disease is less well understood. Extensive genetic and experimental evidence have underscored the importance of the PI3K-PTEN-AKT signaling pathway, not only in genesis (3-5) but also in progression (6, 7) of PCA. In addition, specific genetic events, such as androgen receptor mutation or amplification, Bcl2 activation, and/or loss of p53 tumor suppressor function, had been associated with transition to AI disease (5, 8-16).

In contrast, the role of activated RAS-RAF-MAPK signaling in PCA is less well-established, although a growing body of evidence has pointed to the pathogenetic relevance of this pathway in prostate cancer biology. First, MAP kinase activation has been shown to correlate with disease progression in human PCA specimens (17). Second, virtually all AI xenografts exhibit elevated phosphor-MAP kinase levels and RAS activation renders LNCaP cells less dependent on androgens *in vitro* (18). Furthermore, analysis of various RAS effector mutants with differential capacity to engage specific downstream signaling pathways has also highlighted the MAPK axis in reducing androgen-dependence of LNCaP cells. Third, activating mutations in all three RAS family members have been reported in human PCA specimens (58), primarily from Japanese men, wherein these early studies reported a 13-30% frequency of mutations (19-23). More recently, in a study of Korean cases, KRAS activating mutations were detected in 7% of cases and another 10% harbored the $BRAF^{V600E}$ activating mutation (24). In line with these mutation data, Raf1 expression is often found to be elevated and B-Raf inhibitor expression reduced in human prostate tumors (25). Lastly, ETV1/ER85, a partner in the high frequency TMPRSS2:ETV1 chromosomal fusion event in human prostate cancer, is a downstream target of RAS-RAF-MAPK signaling (26). These reinforcing, albeit correlative, data have implicated activated RAS-RAF-MAPK signaling in the prostate cancer genesis and progression.

Histopathologically, the majority of human PCA are adenocarcinomas derived from glandular epithelium, initiating as prostatic intraepithelial neoplasia (PIN), which progresses to locally invasive adenocarcinoma and metastasis. The prostate gland is composed of two major epithelial cell types: luminal and basal epithelial cells which arise from the urogenital sinus epithelium (UGE). The luminal epithelia are columnar secretary cells which serve as the major functional component of the prostate gland and express prostate-specific markers such as androgen receptor, Nkx3.1 and prostate-specific secretory proteins (10, 27). The basal epithelia reside along the basement membrane and express markers in common with basal epithelial cells in other epithelial tissues including cytokeratin 14 and p63 (10, 27). Recent work has supported the view that the p63+ basal cells are progenitor cells required for maintaining prostate ductal integrity, as well as differentiation and survival of secretory luminal cells (28-30). Whether basal and/or luminal cells serve as the cell-of-origin for prostate adenocarcinoma remains an area of active investigation.

Genetically engineered mouse (GEM) models have enabled the validation and functional analysis of several key genetic alterations found in prostate cancer development (reviewed in (31, 32). The majority of invasive PCA GEM models have largely emphasized AKT activation strategies such as *myr-AKT* or *Pten* deletion, alone or together with *p53* or *p27* inactivation (3-5, 8, 33-35). Other well-established models include prostate-specific expression of *c-Myc* or SV40 oncogenes (1, 36, 37). Of relevance to our study, it is worth noting that these oncogene-driven GEM models have utilized the androgen-responsive probasin promoter to target transgene expression to the prostatic epithelium. The androgen-responsive nature of this promoter permits androgen dependent tumorigenicity but complicates the analysis of AI progression mechanisms.

Previously, in the course of modeling $HRAS^{V12}$-driven melanomas in the mouse, we unexpectedly observed occasional invasive prostate cancers in a handful of mice that did not develop lethal melanomas (LC, unpublished observations). In this inducible bitransgenic system, possessing both tyrosinase-driven tetracycline activator (Tyr-rtTA) and RAS reporter (Tet-$HRAS^{V12}$) transgenes on Ink4a/Arf-/- background (38), we documented fortuitous expression of the Tyr-rtTA transgene in the prostatic epithelium (see below). Recognizing the potential of this inducible and AR-independent transgenic system, we engineered mice with

targeted expression of $BRAF^{V600E}$, the most potent activator of the RAS-MAPK signaling and a mutation observed in about 10% of human PCA (24), to the prostate epithelium. With this model, we sought genetic evidence for whether activation of MAPK signaling via BRAF mutation plays causal and maintenance roles in prostate tumorigenesis.

**Results**

***BRAF* activation drives aberrant proliferation in p63+ basal epithelial cells of the prostate.***

The occurrence of prostate cancers in tyrosinase promoter/enhancer-driven transgenic mice prompted a detailed analysis of transgene expression in the prostate. Examination of transgene expression was performed in all 3 lobes of the prostate glands in 8-week-old bi-transgenic iBRAF* males (iBRAF*, short for "*Tyr-rtTA::Tet-BRAF*::Ink4a/Arf-/-*"). We detected *BRAF** transcripts in all 3 lobes of iBRAF* mice on doxycycline (n=2 mice examined), but not in whole prostate glands derived from WT or iBRAF* transgenic males off doxycycline using transgene-specific RT-PCR (Fig. 1*A*; n=2 for each). As RNA *in situ hybridization* (RISH) of BRAF detects both endogenous *BRAF* and transgene *BRAF** expression throughout the prostatic epithelium (data not shown), we tracked transgene *BRAF** expression by *rtTA* RISH (*nb*., *rtTA* is foreign to the mammalian genome). Upon doxycycline exposure, rtTA is known to potently drive expression of a transgene linked to a Tet-responsive promoter and is therefore a highly specific read-out of the Tet-driven transgene (*BRAF** in this case) expression. *rtTA* transcripts were not detected in non-transgenic wild-type prostate gland, yet were abundant in iBRAF* transgenic prostates exposed to doxycycline (Fig. 1*B*), particularly in the luminal cells (Fig. 1*B*, zoom-in panel, see arrows). To further refine localization of transgene expression in the epithelium and determine whether the transgene is also expressed in the basal cell compartment, we performed serial p63 IHC and *rtTA* RISH (see Materials & Methods) in 8-week-old male iBRAF* prostate glands induced on doxycycline (Fig. 1*C*). Indeed, *rtTA* transcripts were found in both p63+ basal cells and luminal cells (approximately 50% of the p63+ basal cells showed stronger *rtTA* expression; see arrows), indicating that this transgenic system can target expression to both the basal progenitor and the luminal compartments of prostate glands.

To examine the functional impact of *BRAF** transgene expression in the prostate, we monitored doxycycline-dependent proliferative responses in histologically normal prostates of iBRAF* and control mice. These analyses revealed enhanced epithelial proliferation documented by increased Ki67 index from 2.25 (+/- 0.83) per 100 nuclei in 8-week-old WT to 6.9 (+/- 0.95) per 100 nuclei in age-matched iBRAF* prostate (n=

300 nuclei/area x 5 areas counted in each sample; p = 0.00035; Fig. 1*D*). Notably, this BRAF*-induced proliferative response was more prominent in the basal cell compartment, as evident by the observation that most of the strong Ki67 positive signals were confined to p63+ cells (Fig. 1*E*; approximately 50% of p63+ basal cells in iBRAF* prostate glands were positive for Ki67).

***iBRAF* mice developed AKT-independent invasive adenocarcinoma of the prostate.***

A serial histopathological examination of the prostates from iBRAF* transgenic males was conducted to assess the long-term consequences of sustained BRAF* expression in the prostate epithelium. After 5 weeks of iBRAF* induction in 8-week-old animals (left panel in Fig. 2*A*), the prostate gland appeared largely normal although moderate aberrant proliferation was already evident (Fig. 1*E*). Basaloid hyperplasia became evident in 16-week-old mice (middle panel in Fig. 2*A*), consistent with prominent proliferative responses in the basal compartment (Fig. 1*E*), followed by emergency of frank adenocarcinoma by 24 weeks of age (right panel in Fig. 2*A*). Careful follow-up and characterization of a large colony of iBRAF* and control mice showed that only iBRAF* males on doxycycline were prone to PCA development with high penetrance. In founder line #29, 21/34 bi-transgenic iBRAF* males on doxycycline (ON) developed prostate tumors with an average latency of 24 weeks (SD = ± 6 weeks) (Fig. 2*B*, SI Table 1). In comparison, all iBRAF* mice off doxycycline (OFF, n = 10) and single transgenic Tet-BRAF* mice (e.g. *Tet-B-RAF*::Ink4a/Arf-/-*) on doxycycline (ON, n = 9) remained PCA free (SI Table 1). Similar observations were made in a smaller cohort derived from founder line #13 where 3/10 doxycyline-treated iBRAF* males developed PCA with a latency of 23 ± 6 weeks (SI Table 1). Additionally, *BRAF** transgene expression could be documented in these PCA tumors by RT-PCR and RISH (SI Fig. 8); data not shown for RISH).

iBRAF* PCA tumors were rapidly growing, reaching large size and causing local obstruction (Fig. 2*C*). Consistent with its aggressive nature, iBRAF* tumors exhibited epithelial-mesenchymal transition (EMT) associated with downregulation of E-cadherin at the transition from ductal to spindle morphology in these tumors (Fig. 2*D*, compare asterisk to arrow). By high-spatial resolution MRI, PCA could be readily discerned

by the appearance of an enlarged, heterogeneous mass often compressing the bladder (Fig. 2*E*-b, dashed outline; see panel *E*-a for normal prostate size marked by blue highlight). As in human patients, these large lesions caused bladder outlet obstruction and hydronephrosis – distention of the kidney due to outflow obstruction (Fig. 2*E*-c yellow arrow) – with consequent renal failure as a likely cause of mortality.

The complex and context-specific interactions between RAS and PI3K signaling components coupled with the well-documented prominence of PI3K-PTEN-AKT aberrations in PCA, prompted analysis of downstream signaling events in a collection of iBRAF* PCA tumors. Consistent with the known ability to BRAF* to potently activate MAPK signaling, all iBRAF* tumors showed p-ERK activation by Western blot and IHC analyses (Fig. 5*A* and *B*). Notably, while Western blot analysis of *Pten*-null PCA showed strong AKT and S6-Kinase activation, none of the iBRAF* tumors examined showed AKT activation yet sustained S6-Kinase activation (Fig. 5*A*). IHC analysis of additional iBRAF* prostate tumors (n=17) mirrored these Western blot results, showing absence of AKT activation and readily detectable p-S6K immunoreactivity (Fig. 5*C*). Thus, activated BRAF* expression targeted to prostate epithelium in the context of *Ink4a/Arf* deficiency triggers a proliferative response in the basal p63+ compartment, which when sustained, progresses with high penetrance to basaloid hyperplasia and ultimately invasive adenocarcinoma, without requirement of concomitant AKT activation.

***iBRAF* prostate tumors are epithelial***

Given the complex histopathological presentation of the tumors, we utilized a suite of validated prostate lineage markers to determine the origin of these iBRAF* tumors. As shown in Fig. 3, androgen receptor (AR) and Nkx3.1 are expressed in both ductal and spindled components. Nkx3.1 is the earliest known differentiation marker of the prostate luminal epithelium (10), and interestingly its expression was significantly reduced or absent in the spindled cell region of the tumors, possibly reflecting a less differentiated state. Basal cell markers, cytokeratin (CK) 14 and p63 were strongly positive, especially in the ductal components, as was CK19, a marker for transit-amplifying or intermediate differentiated cell (42, 43). This epithelial markers

profile, coupled with negative immunoreactivity to chromogranin and synaptophysin, two markers of neuroendocrine cells (41) (SI Fig. 9), indicates that iBRAF* PCA are epithelial tumors.

To functionally document the epithelial nature of iBRAF* PCA, we utilized the tissue recombinant approach pioneered by Cunha and colleagues (44). Here, recombinant of epithelium from iBRAF* or wildtype mice was mixed with mesenchyme tissues from mice or rats (Fig. 4*A* for design) then grafted under the kidney capsules of adult nude male mice. Grafts were harvested 6 weeks later. As shown in Fig. 4*B*, Recomb A grafts (comprising iBRAF* epithelium and rat mesenchyme) were significantly larger than Recomb B grafts (the converse) from nude mice supplemented with doxycycline drinking water (Fig. 4*B* left panel). On the other hand, without doxycycline, Recomb A grafts were normal in size (Fig 4*B* right panel). Histological analysis of these grafts confirmed basaloid hyperplasia and PIN in grafts from Recomb A ON doxycycline only, while Recomb B grafts from the same hosts or Recomb A from hosts without doxycycline showed normal glandular structure that was indistinguishable from the Recomb C and D controls (Fig. 4*C*). These doxycyline-induced hyperplastic and PIN lesions from Recomb A ON doxycycline grafts exhibited similar marker profile as described for tumors from the *de novo* transgenic mice - positive for Nkx3.1, AR, CK19, CK14 and p63 (SI Fig. 10; data not shown for CK19 and CK14) as well as evidence for significant expansion of the p63+ compartment (SI Fig. 10). On the biochemical level, a profile of robust p-ERK and p-S6K activation without detectable p-AKT activity was observed in these tissue recombinant specimens similar to tumors from *de novo* transgenic mice (Fig. 5C right panel and data not shown for p-ERK). In summary, lineage marker characterization of *de novo* transgenic tumors, coupled with the functional data in the tissue recombinant system, provides clear evidence that *iBRAF** PCA are invasive adenocarcinomas expressing luminal, intermediate and basal cell markers.

***iBRAF* PCA progress to indolent androgen-independent tumors after castration.***

Emergence of androgen-independence represents the most significant disease process in human PCA from the standpoint of mortality, prompting us to determine whether the iBRAF* model develops androgen

independent (AI) tumors. To this end, we identified 10 iBRAF* mice with documented PCA by MRI screening for heterogeneous mass in the prostate gland (representing PCA) for castration. Despite frequent bladder irrigation in an effort to relieve outlet obstruction, 50% (n=5) animals succumbed peri-operatively which was likely due to a generally compromised physiological state secondary to renal failure. Of the surviving animals, two were sacrificed at one-week post-castration (#36 and #57) and the remaining 3 were followed by weekly MRI for 4 weeks. Volumes of the prostate mass in all 5 mice decreased during the observation period (Fig. 6*A* and SI Fig. 11) but histopathological examination identified residual tumor nodules in two of the five castrated iBRAF* mice (#46 and #57). These tumor nodules were AR+ and p63+ with strong p-ERK and p-S6K activation but without detectable p-AKT (Fig. 6*B*). That they were comprised of viable malignant cells was shown by low apoptosis indice, comparable with index observed in pre-castrated tumor (Fig. 6*C*). However, compared to the rapidly growing pre-castration tumors, these post-castrated tumors were indolent, with proliferation indices of 6.8 (+/-3.6) and 6.2 (+/-2.2), respectively, compared to an index of 26.6 (+/-3.6) in the pre-castrated tumors (n= 300 nuclei/area x 5 areas counted in each sample; $p < 0.001$ for both; Fig. 6*C*). Thus, it appears that BRAF driven ERK and S6K activation alone is not sufficient to drive androgen-independent growth post castration, although it appears to be permissive of survival in low androgen state.

***BRAF activation is not required for iBRAF* PCA maintenance.***

To determine whether constitutive BRAF* signaling is required for iBRAF* tumor maintenance, we performed doxycycline withdrawal study in iBRAF* transgenic animals with documented PCA by MRI or by physical examination. First, two iBRAF* mice were identified as tumor-bearing and enlisted into serial MRI after doxycycline was removed from the drinking water. Unexpectedly, tumors continued to grow in both animals as shown on MRI (Fig. 7*A*), requiring termination and sacrifice of ZD839 at one week and ZD835 at 4 weeks post doxycycline withdrawal. Similarly, two additional iBRAF* mice with tumors by palpation were taken off doxycycline; close follow-up revealed continued tumor growth, requiring sacrifice at 2 weeks and 4 weeks, respectively (data not shown). These off-doxycycline tumors did not express BRAF* by Western blot

analysis (Fig. 7*B*) or by IHC (Fig. 7*C*, compare immunoreactivity to left panel). Accordingly, ERK phosphorylation was undetectable in ZD839 and only patchy in ZD835. Consistent with its continued growth *in vivo*, robust Ki67 and minimal TUNEL staining was documented in these off-doxycycline tumors, similar to the profile of on-doxycycline iBRAF* PCA. Corroborating with this was the finding that pharmacological inhibition of MEK with CI-1040 in renal capsule grafts of iBRAF* tumors (n=2) did not inhibit tumor growth despite extinction of pERK activities (SI Fig. 12). Taken together, these observations indicate that, while sustained BRAF* activation in the prostate gland is sufficient to drive development of AKT-independent invasive prostate adenocarcinoma, it is not required for maintenance of established PCA.

**Discussion**

This study, together with recently reported BRAF mutations in human prostate tumors (24), demonstrates the pathogenetic relevance of MAP kinase activation in prostate tumorigenesis. By targeting BRAF V600E – a human-relevant mutation known to potently activate MAP kinase – to the mouse prostate epithelium, we show here that MAP kinase activation can drive aberration proliferation and basaloid hyperplasia, leading to emergence of AKT-independent invasive adenocarcinoma of the prostate gland with short latency and high penetrance. The profile of strong ERK and S6K activation in the absence of AKT in iBRAF* tumors is consistent with the model proposed by Pandolfi and colleagues, whereby constitutive ERK activation inhibits TSC complex and subsequent activation of mTOR and downstream S6K (46). Gratifyingly, among four $BRAF^{V600E}$ mutated human PCA (21, 23, 24) with strong pERK and pS6K activation by IHC, weak to absent pAKT immunoreactivity was observed in two (#S04-7014 and #S04-7989 in SI Fig. 13), supporting the notion that this *iBRAF** transgenic system is modeling a subset of human PCA.

In both mouse and human systems, activation of both AKT and ERK signaling is commonly observed during the initiation and progression of PCA (25, 52). Since most mouse prostate cancer models are driven by AKT-activation, independent contribution of MAPK activation to prostate turmorigenesis has been difficult to establish. Here, by demonstrating that evolution from benign hyperplasia to invasive prostate tumors does not require concomitant AKT activation, this *iBRAF** model offers the first genetic proof that MAPK activation alone is sufficient for initiation and progression to invasive PCA *in vivo*. Additionally, the ability to enforce MAPK activation via mutant BRAF expression under an androgen-insensitive promoter renders this *iBRAF** model an ideal system for genetic dissection of MAPK contribution independent of AKT during AI progression. While they grow rapidly in androgen-rich conditions, these AKT-negative *iBRAF** PCA undergo complete or significant regression upon castration. Those indolent lesions surviving castration remain pAKT negative, pointing to its dispensability for survival in low-androgen state but requirement for AI growth *in vivo*, in line with recent study in *ex-vivo* manipulated system (25). Thus, we conclude that while it may be permissive for survival post castration, BRAF driven MAPK activation is not sufficient to drive active AI growth under an

androgen-limited state.

Finally, while MAPK activation alone can initiate prostate tumorigenesis, continued mutant BRAF expression or downstream MAPK activation is not required for maintenance of established PCA. Genetic inactivation of BRAF* by doxycycline withdrawal in 4 BRAF*-driven tumors did not lead to tumor growth inhibition nor regression. Pharmacological inhibition of MEK similarly failed to inhibit growth of renal capsule tumor grafts. Taken together, these observations indicate that continued expression of mutant BRAF or activation of MAPK is not required to sustain growth or maintain viability of established PCA. This contrasts with findings in BRAF*-driven lung adenocarcinoma model where BRAF* acts not only as an initiating oncogene but shown to be required for maintenance (57), highlighting the context/lineage specific role(s) of an oncogenic event in genesis, progression and maintenance.

In summary, we describe here a novel genetically engineered mouse model of AKT-independent invasive PCA driven by MAPK activation via inducible BRAF mutation under an androgen-insensitive promoter. This model serves as a unique system for dissecting contribution of MAPK, relative to AKT, in development, progression and treatment of PCA.

**Acknowledgements**

We thank Dr. R.A. DePinho for critical reading of the manuscript and members of the laboratories for helpful discussion.

**Grant support:** J.H. Jeong and I. Guney are supported by DOD Prostate Cancer Training Awards. M.F. Loda is supported by NIH PO1 CA089021, Prostate Cancer Foundation Award and DFCI-Novartis Investigator award. W.C. Hahn is supported by NIH PO1 CA089021, Prostate Cancer Foundation Award. C. Abate-Shen is supported by NIH RO1 CA076501 and UO1 CA084294. R. Weissleder and all imaging studies are supported by NIH R24 CA92782, P50 CA86355, and U54 CA119349. This work is supported by grants from the NIH (UO1 CA84313; RO1 CA93947) to L. Chin.

**Materials and Methods**

**Generation of inducible BRAF* (iBRAF*) transgenic mice.** A human wild-type BRAF cDNA was cloned into a pBKS plasmid with its expression under the control of a minimal promoter containing multimerized tet-operons. A constitutively active form of mutant $BRAF^{E600}$ was generated from the pBSK plasmid using QuikChange® Site-Directed Mutagenesis Kit (Stratagene) (designated Tet-$BRAF^{*}$). The Tet-$BRAF^{*}$ construct was injected into oocytes derived from *Ink4a/Arf* null mice. Transgenic mouse lines harboring the Tet- $BRAF^{*}$ elements were crossed with another transgenic mouse lines expressing the reverse tetracycline transactivator under the control of the tyrosinase promoter/enhancer elements (designated Tyr-rtTA) to produce cohorts of single (Tet-BRAF*) and double (designated iBRAF*, Tet-BRAF*; Tyr-rtTA) doxycycline-supplemental drinking water to induce transgene $BRAF^{E600}$ expression as previously described (38).

**Transplantation of tissue recombinants.** A two-way tissue recombination was performed. Mouse and rat embryonic urogenital sinuses were obtained at 16.5 days post coitum (dpc) and 18.5 dpc, respectively, as described previously (44). After treatment of trypsin, epithelium and mesenchyme were separated under the microscope. Next, mouse urogenital sinus epithelium (mUGE) and rat urogenital sinus mesenchyme (rUGM), or mouse urogenital sinus mesenchyme (mUGM) and rat urogenital sinus epithelium (rUGE), were combined. Tissue recombinants were grafted under the kidney capsules of adult male nude mouse host for 6 weeks (with doxycycline on or off). Upon harvesting the grafts, tissues were fixed in 10% formalin overnight, and processed for histology and immunostaining.

**Histology and immunohistochemistry.** All the tissue samples were fixed in 10% formalin overnight and embedded in paraffin. Immunohistochemistry were performed as described previously (53). For antigen retrieval, slides were heated in 0.01 M citrate buffer (pH 6.0) in the microwave four times at four minutes each time. The antibodies and dilutions are: BRAF, 1:250 (Santa Cruz); phospho-Erk, 1:250 (Cell Signaling); Androgen Receptor, 1:250 (ABR); Ki-67, 1:2000 (Novacastra); Cytokeratin-14, 1: 50 (Biogenex); p63, 1:600 (Santa Cruz); Chromogranin A, 1:4000 (Diasorin); Synaptophysin, 1:500 (Santa Cruz); phospho-p70 S6 kinase 1:250 (Cell Signaling); E-cadherin, 1:250 (transduction lab); phospho-AKT(Ser473), 1:100 (Cell Signaling);

Nkx3.1, 1:6000 (kindly provided by Dr. Cory Abate-Shen ); and Cytokeratin 19, 1:20 (kindly provided by Dr. Nabeel Bardeesy). Apoptotic cell death was detected using the ApopTag® Plus Peroxidase *In Situ* Apoptosis Detection Kit (Chemicon).

**RNA In-situ hybridization (RISH).** The 10% formalin-fixed, paraffin-embedded slides were used for in situ hybridization with DIG-labeled riboprobe. DIG-labeled RNA probes were synthesized from a pBKS plasmid containing a rtTA PCR product (500bp) using either T7 (for sense probe) or T3 (for anti-sense probe) promoter by in vitro transcription system with DIG RNA Labeling Mix (Roche Molecular Biochemicals, Mannheim, Germany). After deparaffinization, slides were digested in proteinase K solution (50 ug/ml) for 10 minutes at 37$^{O}$C. DIG-labeled rtTA RNA probes were diluted in hybridization buffer at the concentration of 1 ug/ml. 100 ul of the diluted RNA probes was added on each slide and covered by 24x 40 mm$^2$ coverslip. Slides were hybridized at 60$^{O}$C overnight, and washed at 65$^{O}$C for 15 minutes twice in 2X SSC buffer with gentle agitating. After the treatment of RNAse A (10 ug/ml) for 30 minutes at 37 $^{o}$C, the slides were washed for 10 minutes twice at room temperature (RT) in 2X SSC buffer and followed by additional washing for 30 minutes twice at 65$^{O}$C in 0.2X SSC buffer with gentle agitation. The slides were washed in PBS for 15 minutes twice at RT and then incubated with anti-Digoxigenin antibody conjugated with alkaline phosphatase (1:2000, Roche) overnight at 4 $^{o}$C. Color was developed by dipping the slides in NTB/BCIP solution (54) approximately for two to four hours in the dark.

For the dual staining, first with immunohistochemical staining procedure, the quick incubation of the slides with antibody against p63 for 10 minutes was performed, and then followed by RNA in situ hybridization procedure with rtTA RNA probe as mentioned above.

**MRI methods.** Magnetic resonance imaging was performed on a 4.7 T on a Bruker imaging system (Pharmascan, Karlsruhe, Germany). Protocols included a Tri-plane and coronal proton density weighted localizer. Multi-slice T2-weighted imaging was performed in the coronal and axial planes utilizing the following parameters: Flip angle = 90°; Matrix size (256 x 256); TR = 2500msec; TE = 44.6ms; field of view

(FOV) = 4.24 x 2.12 cm, slice thickness = 1.2mm. T1-weighted imaging was performed in the coronal and axial planes following the administration of intraperitoneal Gd-DTPA utilizing the following parameters: Flip angle = 90°; Matrix size (256 x 256); TR = 700msec.; TE = 14msec.; field of view (FOV) = 4.24 x 2.12 cm, slice thickness = 1.2mm. Tumor volumes were determined by region of interest (ROI) analysis of T1-weighted post Gd-DTPA enhanced images using robust image analysis software (Osirix®). The sum of the region of interests was multiplied by the slice thickness to obtain tumor volumes. Tumor volumes are reported in cubic centimeter (cc).

**Molecular analysis.** RNA was isolated from the prostate tumor samples, and reverse-transcribed to cDNA as described previously (53). A RT-PCR primer pair for the detection of transgene-specific BRAF expression was as follows (210-bp fragment):

RTM-BRAF-5F: 5'-TCTTCATGAAGACCTCACA-3'

RTM-BRAF-5R: 5'-ACTGTCCAGTCATCAATTCA-3'

PCR amplification condition was 95 °C for 15 min followed by 95 °C for 1min, 62 °C for 1 min, and 72 °C for 1 min with 31 cycles. As an internal control for RT-PCR, ribosomal protein R15 expression was used.

For western blot analysis, tumor lysates were extracted as described previously (53). Total 20 micrograms of lysate was run on 4-12% Bis-Tris NuPAGE (Invitrogen), transferred to PVDF membrane (Perkinelmer), and blotted using the following antibodies: p-ERK, 1:500 (Cell Signaling); phospho-S6 Kinase, 1:500 (Cell Signaling); and p-AKT(Ser473), 1:250 (Cell Signaling).

**Figure Legends.**

**Fig. 1.** Transgene *BRAF** expression in prostate epithelium drives aberrant proliferation of the p63+ prostatic basal cells. (*A*) Transgene *BRAF** transcript was detected in all three lobes (AP, anterior prostate; VP, ventral prostate; DLP, dorsolateral prostate) of the prostate glands from two independent 8-week-old bi-transgenic iBRAF* male mice on doxycycline by transgene-specific RT-PCR. As controls, whole prostate glands were isolated from WT or iBRAF* off doxycycline mice (n=2 for each). Ribosomal protein R15 was used as an internal control for RT-PCR. (*B*) RNA *in situ* hybridization (RISH) using rtTA riboprobe documented expression of *BRAF** transgene in prostate epithelial gland (200X). Arrows indicate the expression of *rtTA* in luminal cell compartment in zoom-in with higher magnification (400X). (*C*) Expression of *BRAF** transgene was detected in both luminal cells and p63+ basal cells of the prostate epithelium of 8-week-old bi-transgenic iBRAF* male mice on doxycycline using dual serial staining of p63 IHC and rtTA RISH. After quick incubation of slides with antibody against p63 for 10 minutes with IHC procedure, RISH procedure with rtTA RNA probe was followed. Brown color for p63+ basal cells by IHC and purple color for *rtTA* expression by RISH were differentially detected by spectro-imaging machine. Note the co-localization of strong *rtTA* expression and p63 immuno-reactivity in approximately 50% of p63+ basal cells (arrows). (*D*) Ki67 staining of histologically-normal prostate glands in 8-week-old males showed increased proliferation index in iBRAF* transgenic (on doxycycline) compared to WT. (*E*) Co-immunofluorescence study in prostate glands isolated from 8-week-old WT and iBRAF* transgenic (on doxycycline) males showed the expansion of p63+ basal cells in the prostate glands of iBRAF* mice. Approximately half of the p63+ cells were in proliferation as measured by co-staining with Ki67 (see arrows).

**Fig. 2.** iBRAF* transgenic males develop invasive adenocarsinoma of the prostate. (*A*) Time-course histological analysis of prostate samples from iBRAF* transgenic mice (on doxycycline) at the indicated ages. Hyperplastic lesions were detected in a 16-week-old iBRAF* transgenic mouse on doxycycline. Up to an age of 24 weeks, approximately 50% of iBRAF* transgenic mice developed PCA. (*B*) Kaplan-Meier analysis of PCA-free survival in iBRAF* (on doxycycline, n=34), iBRAF* (off doxycycline, n=9), and Tet-BRAF* (on

doxycycline, n=10) transgenic males. Only double transgenic iBRAF* mice given doxycycline in their drinking water developed PCA with an average latency of 24 weeks (standard deviation = ± 6 weeks). (*C*) Gross morphology of a prostate tumor from an iBRAF* transgenic mouse. T indicates tumor; B, bladder; and Te, testis. (*D*) The transition from ductal (arrowhead) to spindle (asterisk) morphology is coincident with loss of E-cadherin expression in iBRAF* PCA, consistent with EMT (epithelial-mesenchymal transition). (*E*) Detection of PCA in live mice by MRI. Panel a is a representative image of a WT mouse with normal prostate (highlighted in blue). Panel b is a representative MR image of PCA in an iBRAF* male on doxycycline (red outline; note heterogeneous signals within the lesion). Panel c is a representative MR image of hydronephrosis detected in an iBRAF* mouse with PCA. Note enlarged distended kidney (yellow arrow) in contrast to normal kidney in panel b (green arrow), indicating accumulation of urine in the kidney due to outflow obstruction by the tumor.

**Fig. 3.** iBRAF* prostate tumors exhibit epithelial lineage markers**.** Both ductal and spindled components of iBRAF* prostate tumors express epithelial lineage markers: CK14 and p63 for basal cell, AR and Nkx3.1 for luminal cell, and CK19 for transit-amplifying cells.

**Fig. 4.** iBRAF* embryonic urogenital epithelium drives basaloid hyperplasia in the tissue recombination system. (*A*) Schematic representation of the tissue recombination protocol. Recombinants of iBRAF* transgenic mouse epithelium and rat mesenchyme (Recomb A) were grafted under the right kidney capsules of adult nude mice. The converse recombinants (iBRAF* transgenic mouse mesenchyme and rat epithelium; Recomb B) were also transplanted in the same manner into the left kidney capsule of the same mice. Three of the grafted mice were fed doxycycline drinking water, and two were not. As controls, recombinants of non-transgenic wild-type mouse epithelium and rat mesenchyme (Recomb C) and the converse recombinants (Recomb D) were grafted in the same manner. Grafts were harvested 6 weeks later. (*B*) Macroscopic images show that grafts with Recomb A on doxycycline are larger than both grafts with Recomb B on doxycycline and

grafts with Recomb A off doxycycline. (*C*) Histological analysis of these tissue grafts confirmed basaloid hyperplasia only in grafts with Recomb A on doxycycline, while others showed normal histology.

**Fig. 5.** iBRAF* prostate tumors are AKT-independent. (*A* and *B*) p-ERK activation in iBRAF* PCA tumors (n=5; on doxycycline) was detected by immunoblotting analysis (*A*) and IHC (*B*). In contrast, p-AKT activation was not detected inall iBRAF* PCA tumors (n=5; on doxycycline)**,** although p-S6K activation was more prominent in all iBRAF* PCA tumors (on doxycycline). Control (Ctrl) was a prostate cancer sample from *Pten*-null mouse.. (*C*) p-AKT immunoreactivity was not detected on iBRAF* PCA tumors (n=17) and Recomb A (a recombinant of iBRAF* transgenic mouse epithelium and rat mesenchyme on doxycycline) by IHC, but strong immunoreactivity of p-S6K was still present. PCA sample from *Nkx*3.1-/-, *Pten*+/- compound mutant mice were used as control.

**Fig. 6.** iBRAF* PCA progress to indolent androgen-independence after castration. (*A*) The reduction of tumor volumes was monitored by MRI over a 4-week time course after castration (**a**, tumor (blue) 1 week after castration; **b**, tumor (green) 2 weeks after castration; **c**, tumor (yellow) 3 weeks after castration; **d**, tumor (orange) 4 weeks after castration). Asterisk indicates bladder. (*B*) Histological examination confirmed the presence of prostatic tumor cells in two castrated iBRAF* mice (#46 and #57). The two post-castration tumors were positive for AR (a prostatic luminal cell marker) and p63 (a basal cell marker) by IHC. Also, the post-castration tumor cells were negative for p-AKT, but remained strongly positive for p-ERK and p-S6K on IHC. (*C*) The post-castration tumor cells were viable and growing, not residual tumor remnants, as manifested by low apoptosis index (1.2 (+/-0.45) and 1.4 (+/-0.55) per 100 nuclei for #46 and #57, respectively) on TUNEL, comparable to pre-castration tumor (1.0 (+/-0.71)) (top), and active proliferation by Ki67 staining, albeit at rate much lower than that of pre-castration tumor (6.8 (+/-3.6) and 6.2 (+/-2.2) for #46 and #57, respectively and 26.6 (+/-3.6) in the pre-castrated tumors) (bottom).

**Fig. 7.** iBRAF* prostate tumors do not require BRAF activation for their tumor maintenance. (*A*) Tumor size change was monitored by serial MRI imaging before (baseline; solid line) and after (indicated periods; dotted line) doxycycline withdrawal (7 days for ZD839 and 28 days for ZD835). Yellow line indicates tumor boundary. (*B*) B-RAF expression and p-ERK activation were not detected by immunoblotting analysis in most of off doxycycline iBRAF* PCA tumors (n=3), although one of the off doxycycline iBRAF* tumor samples (ZD835) showed weak p-ERK activation. (*C*) Immunohistological examination using antibodies against B-RAF and p-ERK confirmed the repression of B-RAF* transgene repression during off doxycycline periods (7 days for ZD839 and 28 days for ZD835). However, the tumors were viable and still growing, as manifested by low apoptosis on TUNEL and active proliferation by Ki67 staining.

## References


1. Ellwood-Yen K, Graeber TG, Wongvipat J, et al. Myc-driven murine prostate cancer shares molecular features with human prostate tumors. Cancer Cell 2003;4:223-38.
2. Hill R, Song Y, Cardiff RD, Van Dyke T. Heterogeneous tumor evolution initiated by loss of pRb function in a preclinical prostate cancer model. Cancer Res 2005;65:10243-54.
3. Kim MJ, Cardiff RD, Desai N, et al. Cooperativity of Nkx3.1 and Pten loss of function in a mouse model of prostate carcinogenesis. Proc Natl Acad Sci U S A 2002;99:2884-9.
4. Trotman LC, Niki M, Dotan ZA, et al. Pten dose dictates cancer progression in the prostate. PLoS Biol 2003;1:E59.
5. Wang L, Cunningham JM, Winters JL, et al. BRAF mutations in colon cancer are not likely attributable to defective DNA mismatch repair. Cancer Res 2003;63:5209-12.
6. Mulholland DJ, Dedhar S, Wu H, Nelson CC. PTEN and GSK3beta: key regulators of progression to androgen-independent prostate cancer. Oncogene 2006;25:329-37.
7. Xin L, Teitell MA, Lawson DA, Kwon A, Mellinghoff IK, Witte ON. Progression of prostate cancer by synergy of AKT with genotropic and nongenotropic actions of the androgen receptor. Proc Natl Acad Sci U S A 2006;103:7789-94.
8. Chen Z, Trotman LC, Shaffer D, et al. Crucial role of p53-dependent cellular senescence in suppression of Pten-deficient tumorigenesis. Nature 2005;436:725-30.
9. Bentel JM, Tilley WD. Androgen receptors in prostate cancer. J Endocrinol 1996;151:1-11.
10. Abate-Shen C, Shen MM. Molecular genetics of prostate cancer. Genes Dev 2000;14:2410-34.
11. Stackhouse GB, Sesterhenn IA, Bauer JJ, et al. p53 and bcl-2 immunohistochemistry in pretreatment prostate needle biopsies to predict recurrence of prostate cancer after radical prostatectomy. J Urol 1999;162:2040-5.
12. Bookstein R, MacGrogan D, Hilsenbeck SG, Sharkey F, Allred DC. p53 is mutated in a subset of advanced-stage prostate cancers. Cancer Res 1993;53:3369-73.
13. Navone NM, Labate ME, Troncoso P, et al. p53 mutations in prostate cancer bone metastases suggest that selected p53 mutants in the primary site define foci with metastatic potential. J Urol 1999;161:304-8.
14. Navone NM, Troncoso P, Pisters LL, et al. p53 protein accumulation and gene mutation in the progression of human prostate carcinoma. J Natl Cancer Inst 1993;85:1657-69.
15. Theodorescu D, Broder SR, Boyd JC, Mills SE, Frierson HF, Jr.. p53, bcl-2 and retinoblastoma proteins as long-term prognostic markers in localized carcinoma of the prostate. J Urol 1997;158:131-7.
16. Brewster SF, Oxley JD, Trivella M, Abbott CD, Gillatt DA. Preoperative p53, bcl-2, CD44 and E-cadherin immunohistochemistry as predictors of biochemical relapse after radical prostatectomy. J Urol 1999;161:1238-43.
17. Gioeli D, Mandell JW, Petroni GR, Frierson HF, Jr., Weber MJ. Activation of mitogen-activated protein kinase associated with prostate cancer progression. Cancer Res 1999;59:279-84.
18. Voeller HJ, Wilding G, Gelmann EP. v-rasH expression confers hormone-independent in vitro growth to LNCaP prostate carcinoma cells. Mol Endocrinol 1991;5:209-16.
19. Konishi N, Hiasa Y, Tsuzuki T, Tao M, Enomoto T, Miller GJ. Comparison of ras activation in prostate carcinoma in Japanese and American men. Prostate 1997;30:53-7.
20. Sasaki Y, Niu C, Makino R, et al. BRAF point mutations in primary melanoma show different prevalences by subtype. J Invest Dermatol 2004;123:177-83.
21. Shiraishi T, Muneyuki T, Fukutome K, et al. Mutations of ras genes are relatively frequent in Japanese prostate cancers: pointing to genetic differences between populations. Anticancer Res 1998;18:2789-92.
22. Lin S, Sahai A, Chugh SS, et al. High glucose stimulates synthesis of fibronectin via a novel protein kinase C, Rap1b, and B-Raf signaling pathway. J Biol Chem 2002;277:41725-35.

23. Suzuki H, Aida S, Akimoto S, Igarashi T, Yatani R, Shimazaki J. State of adenomatous polyposis coli gene and ras oncogenes in Japanese prostate cancer. Jpn J Cancer Res 1994;85:847-52.
24. Cho NY, Choi M, Kim BH, Cho YM, Moon KC, Kang GH. BRAF and KRAS mutations in prostatic adenocarcinoma. Int J Cancer 2006;119:1858-62.
25. Gao H, Ouyang X, Banach-Petrosky WA, Gerald WL, Shen MM, Abate-Shen C. Combinatorial activities of Akt and B-Raf/Erk signaling in a mouse model of androgen-independent prostate cancer. Proc Natl Acad Sci U S A 2006;103:14477-82.
26. Tomlins SA, Rhodes DR, Perner S, et al. Recurrent fusion of TMPRSS2 and ETS transcription factor genes in prostate cancer. Science 2005;310:644-8.
27. Schinelli S, Zanassi P, Paolillo M, Wang H, Feliciello A, Gallo V. Stimulation of endothelin B receptors in astrocytes induces cAMP response element-binding protein phosphorylation and c-fos expression via multiple mitogen-activated protein kinase signaling pathways. J Neurosci 2001;21:8842-53.
28. Signoretti S, Pires MM, Lindauer M, et al. p63 regulates commitment to the prostate cell lineage. Proc Natl Acad Sci U S A 2005;102:11355-60.
29. Kurita T, Medina RT, Mills AA, Cunha GR. Role of p63 and basal cells in the prostate. Development 2004;131:4955-64.
30. Tokar EJ, Ancrile BB, Cunha GR, Webber MM. Stem/progenitor and intermediate cell types and the origin of human prostate cancer. Differentiation 2005;73:463-73.
31. Abate-Shen C, Shen MM. Mouse models of prostate carcinogenesis. Trends Genet 2002;18:S1-5.
32. Kasper S: Survey of genetically engineered mouse models for prostate cancer. analyzing the molecular basis of prostate cancer development, progression, and metastasis. J Cell Biochem 2005;94:279-97.
33. Di Cristofano A, De Acetis M, Koff A, Cordon-Cardo C, Pandolfi PP. Pten and p27KIP1 cooperate in prostate cancer tumor suppression in the mouse. Nat Genet 2001;27:222-4.
34. Gao H, Ouyang X, Banach-Petrosky W, et al. A critical role for p27kip1 gene dosage in a mouse model of prostate carcinogenesis. Proc Natl Acad Sci U S A 2004;101:17204-19.
35. Majumder PK, Yeh JJ, George DJ, et al. Prostate intraepithelial neoplasia induced by prostate restricted Akt activation: the MPAKT model. Proc Natl Acad Sci U S A 2003;100:7841-6.
36. Zhang BH, Tang ED, Zhu T, Greenberg ME, Vojtek AB, Guan KL. Serum- and glucocorticoid-inducible kinase SGK phosphorylates and negatively regulates B-Raf. J Biol Chem 2001;276:31620-6.
37. Kasper S, Tu W, Roberts RL, Shappell SB. Transgenic mouse models for prostate cancer. Identification of an androgen-dependent promoter and creation and characterization of the long probasin promoter-Large T antigen (LPB-Tag) model. Methods Mol Med 2003;81:113-47.
38. Chin L, Tam A, Pomerantz J, et al. Essential role for oncogenic Ras in tumour maintenance. Nature 1999;400:468-72.
39. Cavallaro U, Schaffhauser B, Christofori G. Cadherins and the tumour progression: is it all in a switch? Cancer Lett 2002;176:123-8.
40. Batlle E, Sancho E, Franci C, et al. The transcription factor snail is a repressor of E-cadherin gene expression in epithelial tumour cells. Nat Cell Biol 2000;2:84-9.
41. Segawa N, Mori I, Utsunomiya H, et al. Prognostic significance of neuroendocrine differentiation, proliferation activity and androgen receptor expression in prostate cancer. Pathol Int 2001;51:452-9.
42. Hudson DL. Epithelial stem cells in human prostate growth and disease. Prostate Cancer Prostatic Dis 2004;7:188-94.
43. Verhagen AP, Ramaekers FC, Aalders TW, Schaafsma HE, Debruyne FM, Schalken JA. Colocalization of basal and luminal cell-type cytokeratins in human prostate cancer. Cancer Res 1992;52:6182-7.
44. Cunha GR, Donjacour AA, Cooke PS, et al. The endocrinology and developmental biology of the prostate. Endocr Rev 1987;8:338-62.
45. Karasarides M, Chiloeches A, Hayward R, et al. B-RAF is a therapeutic target in melanoma. Oncogene 2004;23:6292-8.

46. Gast A, Forsti A, Soderberg M, Hemminki K, Kumar R. B-RAF mutations in tumors from melanoma-breast cancer families. Int J Cancer 2005;113:336-7.
47. Huss WJ, Gray DR, Werdin ES, Funkhouser WK, Jr., Smith GJ. Evidence of pluripotent human prostate stem cells in a human prostate primary xenograft model. Prostate 2004;60:77-90.
48. Signoretti S, Waltregny D, Dilks J, et al. p63 is a prostate basal cell marker and is required for prostate development. Am J Pathol 2000;157:1769-75.
49. Litvinov IV, De Marzo AM, Isaacs JT. Is the Achilles' heel for prostate cancer therapy a gain of function in androgen receptor signaling? J Clin Endocrinol Metab 2003;88:2972-82.
50. De Marzo AM, Meeker AK, Epstein JI, Coffey DS. Prostate stem cell compartments: expression of the cell cycle inhibitor p27Kip1 in normal, hyperplastic, and neoplastic cells. Am J Pathol 1998;153:911-9.
51. Bachoo RM, Maher EA, Ligon KL, et al. Epidermal growth factor receptor and Ink4a/Arf: convergent mechanisms governing terminal differentiation and transformation along the neural stem cell to astrocyte axis. Cancer Cell 2002;1:269-77.
52. Uzgare AR, Isaacs JT. Enhanced redundancy in Akt and mitogen-activated protein kinase-induced survival of malignant versus normal prostate epithelial cells. Cancer Res 2004;64:6190-9.
53. Aguirre AJ, Bardeesy N, Sinha M, et al. Activated Kras and Ink4a/Arf deficiency cooperate to produce metastatic pancreatic ductal adenocarcinoma. Genes Dev 2003;17:3112-26.
54. Laroche-Joubert N, Marsy S, Luriau S, Imbert-Teboul M, Doucet A. Mechanism of activation of ERK and H-K-ATPase by isoproterenol in rat cortical collecting duct. Am J Physiol Renal Physiol 2003;284:F948-54.
55. Cheng J, Thompson MA, Walker HJ, et al. Differential regulation of mesangial cell mitogenesis by cAMP phosphodiesterase isozymes 3 and 4. Am J Physiol Renal Physiol 2004;287:F940-53.
56. Davies H, Bignell GR, Cox C, et al. Mutations of the BRAF gene in human cancer. Nature 2002;417:949-54.
57. Ji H, Wang Z, Perera SA, et al. Mutations in BRAF and KRAS converge on activation of the mitogen-activated protein kinase pathway in lung cancer mouse models. Cancer Res 2007;67:4933-9.
58. Thomas RK, Baker AC, DeBiasi RM, et al. High-throughput oncogene mutation profiling in human cancer. Nat Genet 2007;39:347-57.

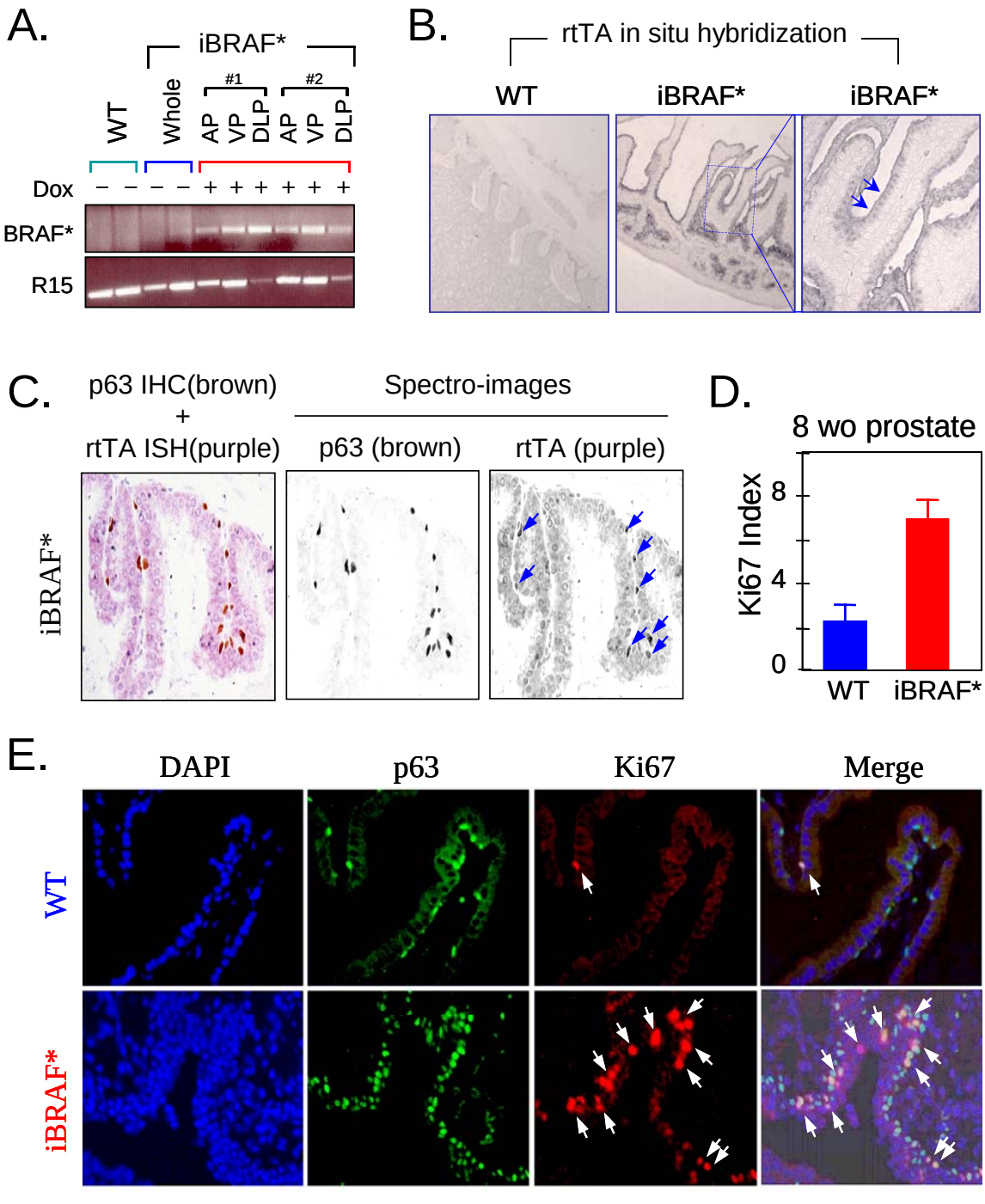
A.
iBRAF*
WT
Whole
#1
AP
VP
DLP
#2
AP
VP
DLP
Dox
BRAF*
R15
B.
rtTA in situ hybridization
WT
iBRAF*
iBRAF*
C.
p63 IHC(brown)
+
rtTA ISH(purple)
Spectro-images
p63 (brown)
rtTA (purple)
iBRAF*
D.
8 wo prostate
Ki67 Index
8
4
0
WT
iBRAF*
E.
DAPI
p63
Ki67
Merge
WT
iBRAF*

Fig. 1.

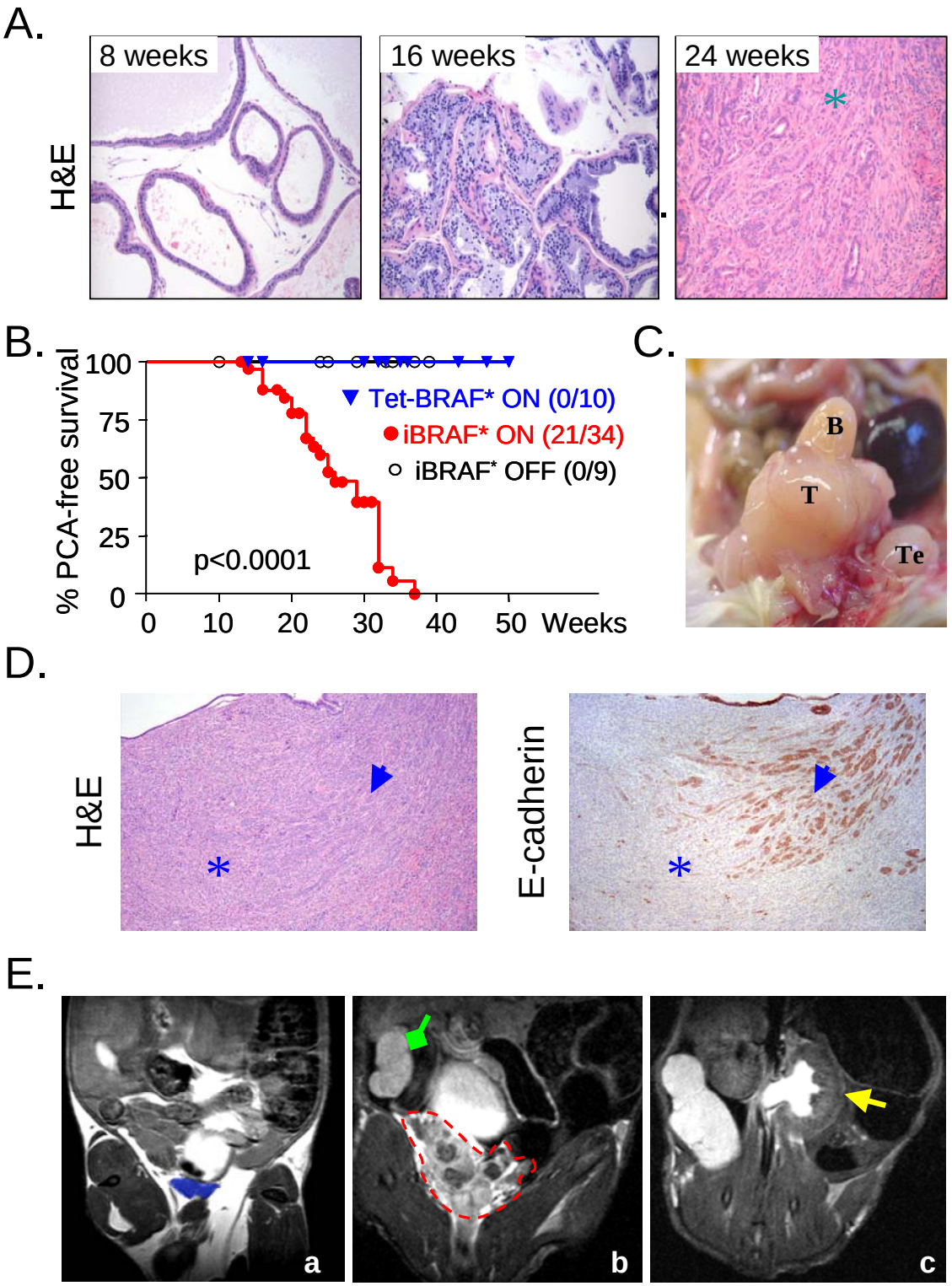
A.
8 weeks
16 weeks
24 weeks
H&E
B.
% PCA-free survival
100
75
50
25
0
0
10
20
30
40
50
Weeks
Tet-BRAF* ON (0/10)
iBRAF* ON (21/34)
iBRAF* OFF (0/9)
p<0.0001
C.
B
T
Te
D.
H&E
E-cadherin
E.
a
b
c

Fig. 2.

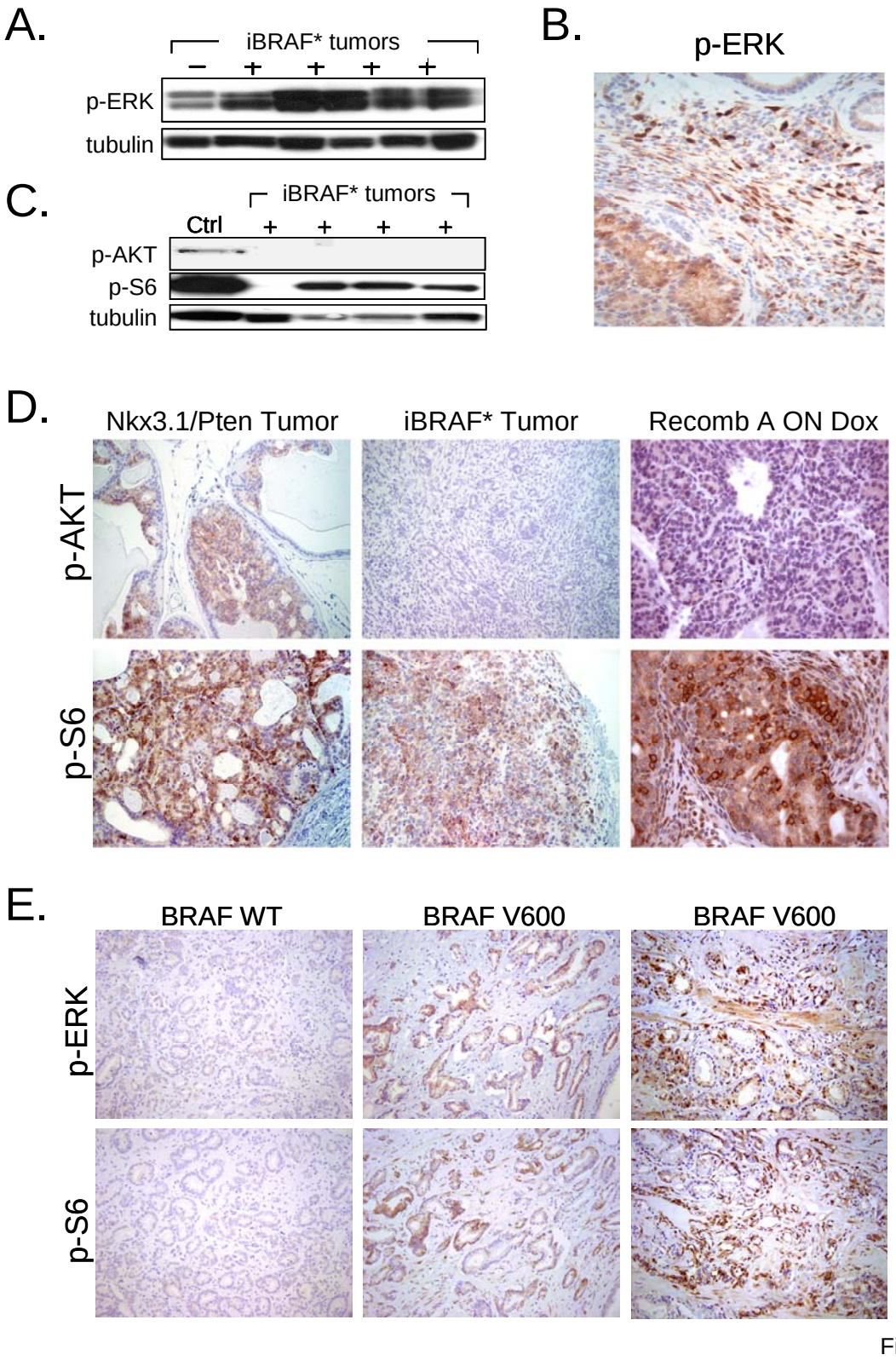
A.
iBRAF* tumors
– + + + +
p-ERK
tubulin
B.
p-ERK
C.
iBRAF* tumors
Ctrl + + + +
p-AKT
p-S6
tubulin
D.
Nkx3.1/Pten Tumor
iBRAF* Tumor
Recomb A ON Dox
p-AKT
p-S6
E.
BRAF WT
BRAF V600
BRAF V600
p-ERK
p-S6

Fig. 3.

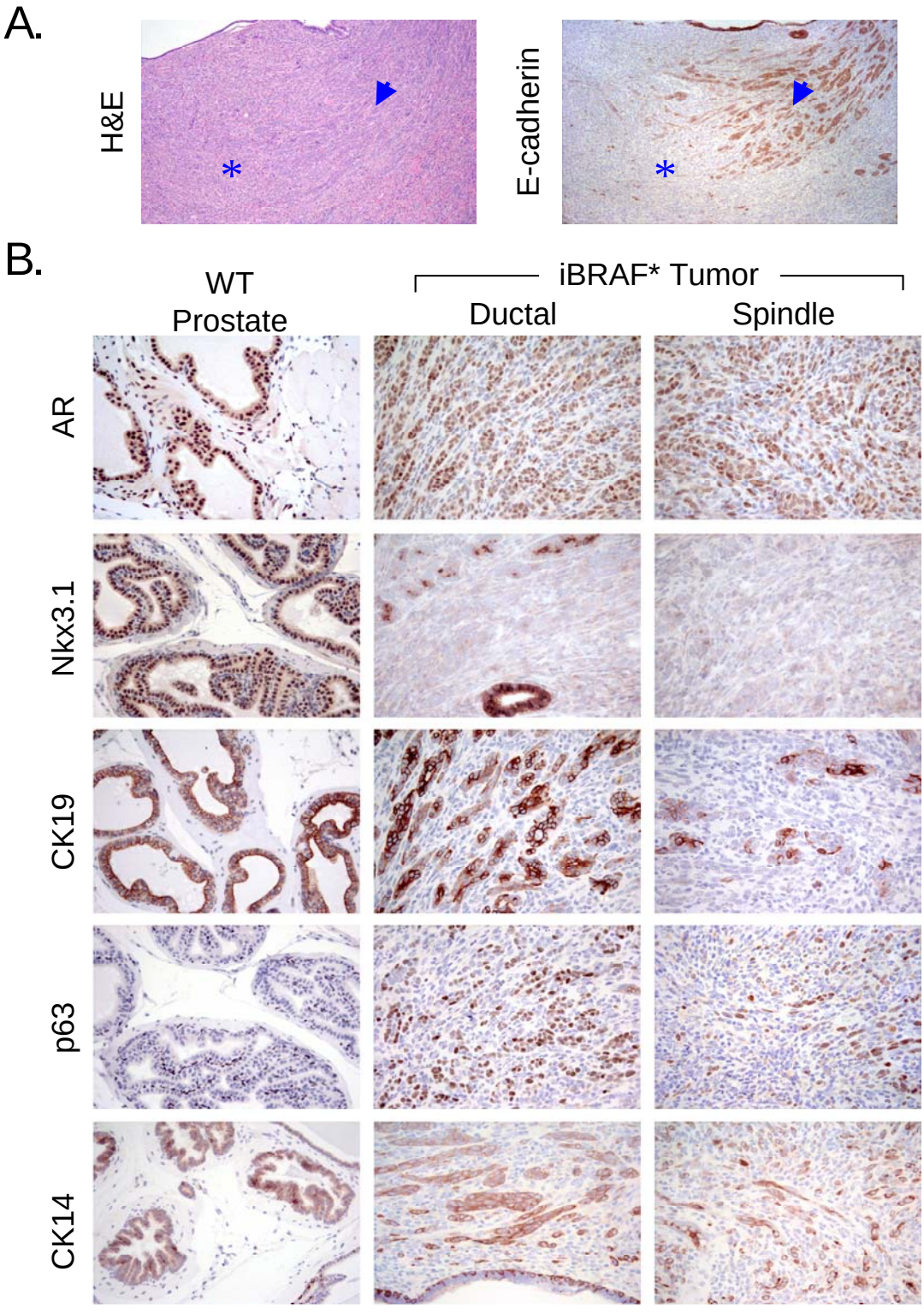
A.
H&E
E-cadherin
B.
WT Prostate
iBRAF* Tumor
Ductal
Spindle
AR
Nkx3.1
CK19
p63
CK14

Fig. 4.

A.

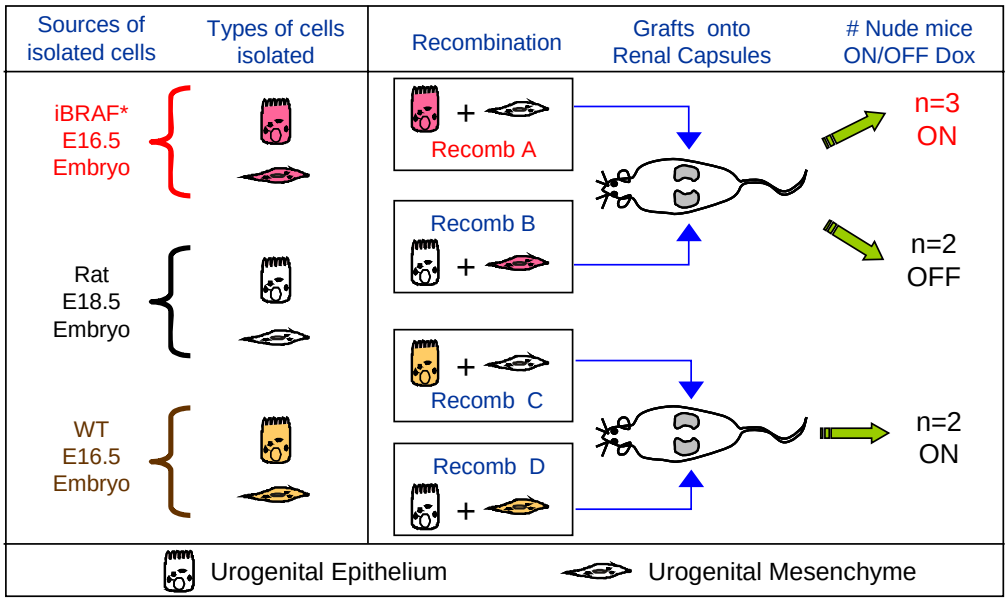
Sources of isolated cells
Types of cells isolated
Recombination
Grafts onto Renal Capsules
# Nude mice ON/OFF Dox
iBRAF* E16.5 Embryo
Rat E18.5 Embryo
WT E16.5 Embryo
Recomb A
Recomb B
Recomb C
Recomb D
n=3 ON
n=2 OFF
n=2 ON
Urogenital Epithelium
Urogenital Mesenchyme

B.


ON doxycycline
OFF doxycycline
ON doxycycline
METRIC
Recomb A
Recomb A
Recomb A
Recomb B

C.

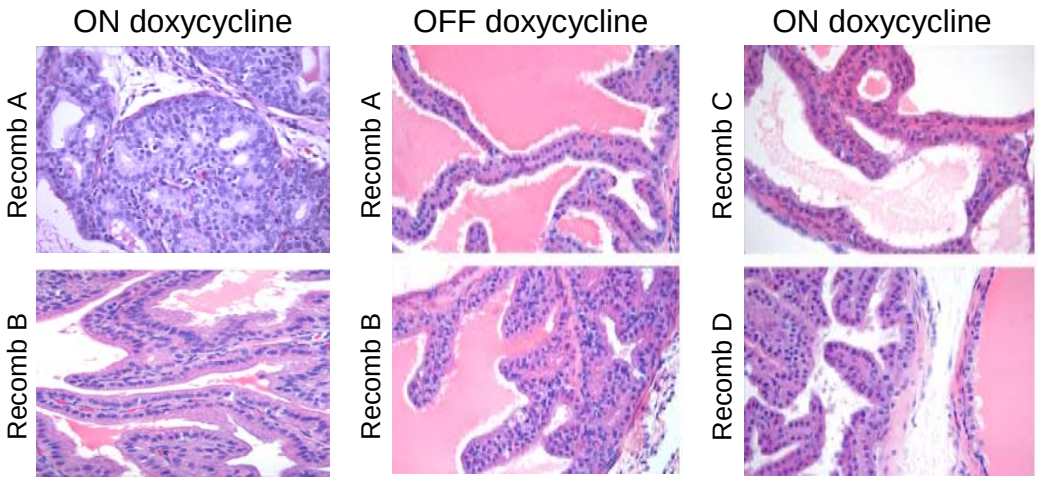
ON doxycycline
OFF doxycycline
ON doxycycline
Recomb A
Recomb B
Recomb A
Recomb B
Recomb C
Recomb D

Fig. 5.

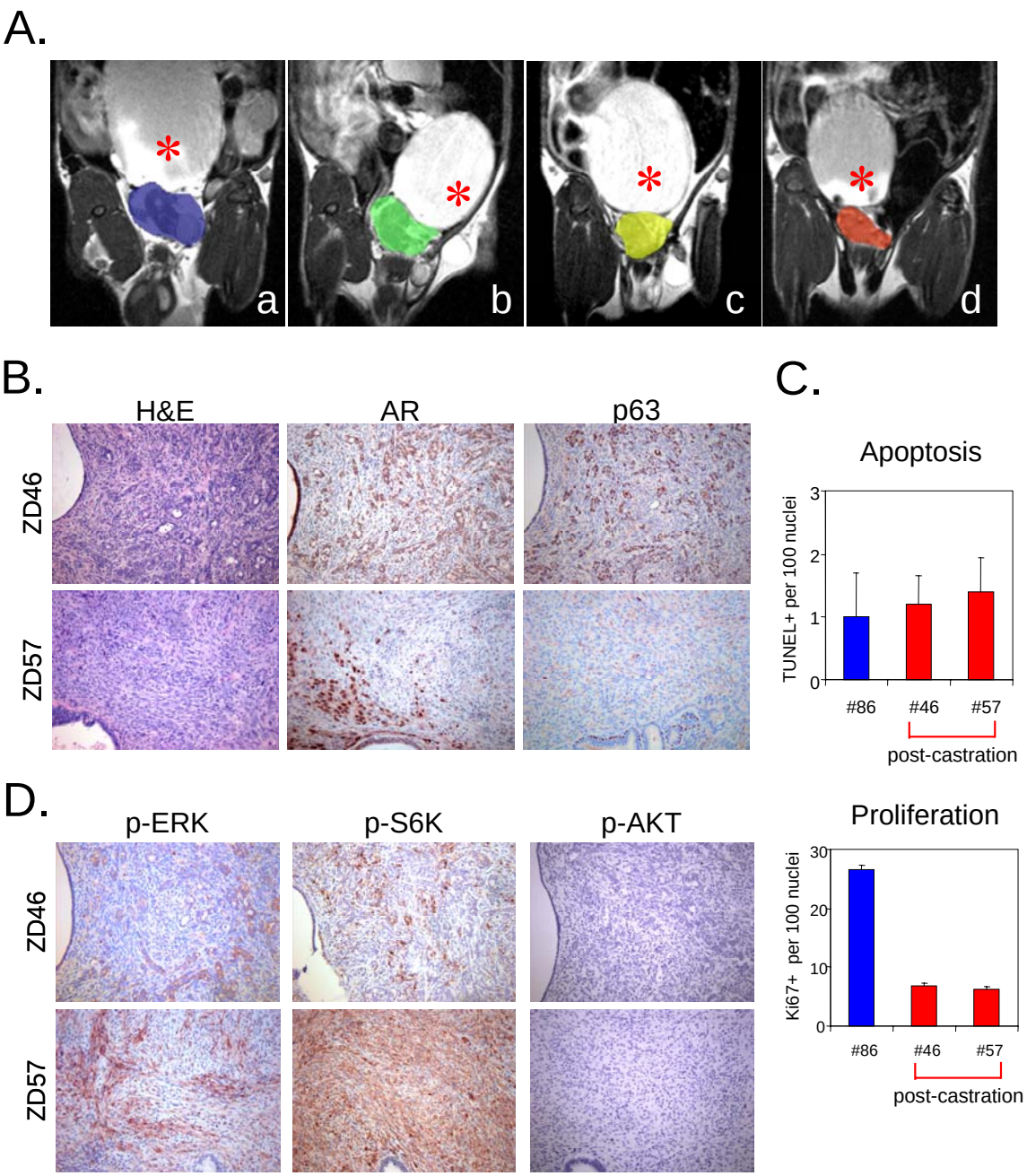
A.
a
b
c
d
B.
H&E
AR
p63
ZD46
ZD57
C.
Apoptosis
TUNEL+ per 100 nuclei
0
1
2
3
#86
#46
#57
post-castration
D.
p-ERK
p-S6K
p-AKT
ZD46
ZD57
Proliferation
Ki67+ per 100 nuclei
0
10
20
30
#86
#46
#57
post-castration

Fig. 6.

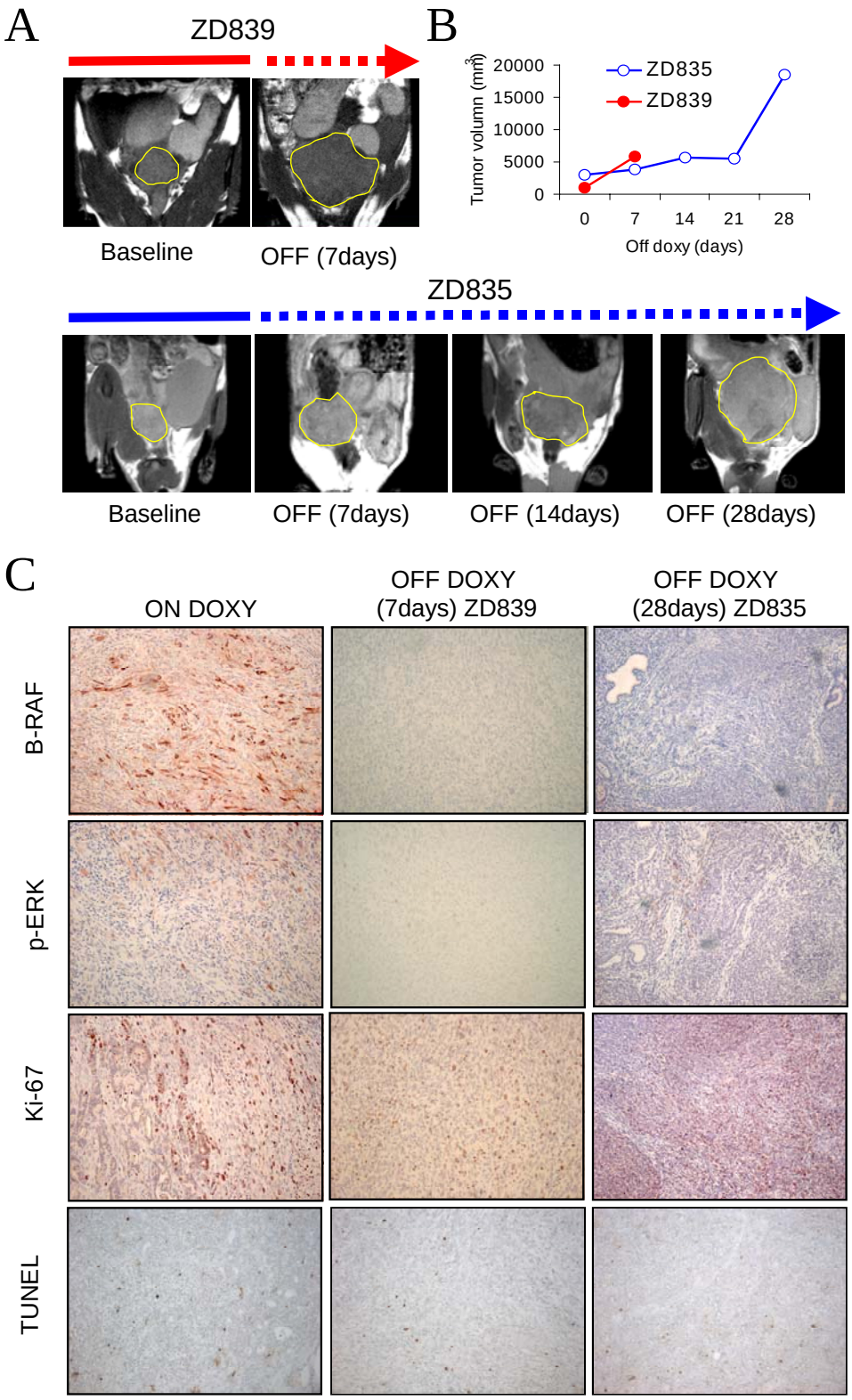
A
ZD839
Baseline
OFF (7days)
B
Tumor volumn (mm3)
20000
15000
10000
5000
0
ZD835
ZD839
0
7
14
21
28
Off doxy (days)
ZD835
Baseline
OFF (7days)
OFF (14days)
OFF (28days)
C
ON DOXY
OFF DOXY (7days) ZD839
OFF DOXY (28days) ZD835
B-RAF
p-ERK
Ki-67
TUNEL

Fig. 7.

**Supplemental Table 1. The summary of phenotypes of iBRAF* transgenic male mice**

**A. Line 29**

| Number | Mouse I. D. | Sex | Genotype | Age of death[c] (weeks) | Doxy | Pheotypes[d] |
|---|---|---|---|---|---|---|
| 1 | 233 | M | iBRAF* [a] | 25 | off | no obvious tumors |
| 2 | 238 | M | iBRAF* | 34 | off | lymphoma |
| 3 | 239 | M | iBRAF* | 10 | off | no obvious tumors |
| 4 | 240 | M | iBRAF* | 29 | off | no obvious tumors |
| 5 | 241 | M | iBRAF* | 34 | off | lymphoma |
| 6 | 423 | M | iBRAF* | 33 | off | sarcoma |
| 7 | 531 | M | iBRAF* | 37 | off | no obvious tumors |
| 8 | 547 | M | iBRAF* | 24 | off | lymphoma |
| 9 | 762 | M | iBRAF* | 39 | off | no obvious tumors |
| 10 | 662 | M | Tet-BRAF* [b] | 35 | on | lymphoma |
| 11 | 731 | M | Tet-BRAF* | 43 | on | sarcoma |
| 12 | 747 | M | Tet-BRAF* | 30 | on | no obvious tumors |
| 13 | 700 | M | Tet-BRAF* | 47 | on | lymphoma |
| 14 | 668 | M | Tet-BRAF* | 50 | on | sarcoma |
| 15 | 761 | M | Tet-BRAF* | 14 | on | no obvious tumors |
| 16 | 794 | M | Tet-BRAF* | 32 | on | no obvious tumors |
| 17 | 862 | M | Tet-BRAF* | 36 | on | sarcoma |
| 18 | 863 | M | Tet-BRAF* | 33 | on | sarcoma |
| 19 | 919 | M | Tet-BRAF* | 16 | on | no obvious tumors |
| 20 | 61 | M | iBRAF* | 37 | on | prostate cancer |
| 21 | 65 | M | iBRAF* | 32 | on | lymphoma |
| 22 | 76 | M | iBRAF* | 25 | on | prostate cancer |
| 23 | 86 | M | iBRAF* | 23 | on | prostate cancer |
| 24 | 102 | M | iBRAF* | 32 | on | prostate cancer |
| 25 | 103 | M | iBRAF* | 18 | on | skin cancer |
| 26 | 111 | M | iBRAF* | 18 | on | lymphoma and sarcoma |
| 27 | 113 | M | iBRAF* | 34 | on | prostate cancer |
| 28 | 137 | M | iBRAF* | 26 | on | prostate cancer |
| 29 | 139 | M | iBRAF* | 29 | on | prostate cancer |
| 30 | 260 | M | iBRAF* | 32 | on | prostate cancer |
| 31 | 516 | M | iBRAF* | 14 | on | prostate cancer |
| 32 | 558 | M | iBRAF* | 22 | on | melanoma |
| 33 | 565 | M | iBRAF* | 22 | on | lymphoma |
| 34 | 584 | M | iBRAF* | 22 | on | prostate cancer |
| 35 | 600 | M | iBRAF* | 16 | on | no obvious tumors |
| 36 | 620 | M | iBRAF* | 21 | on | lymphoma |
| 37 | 623 | M | iBRAF* | 31 | on | skin cancer |
| 38 | 654 | M | iBRAF* | 19 | on | prostate cancer |
| 39 | 831 | M | iBRAF* | 16 | on | prostate cancer |
| 40 | 832 | M | iBRAF* | 16 | on | prostate cancer |
| 41 | 834 | M | iBRAF* | 13 | on | no obvious tumors |
| 42 | 835 | M | iBRAF* | 20 | on | prostate cancer |
| 43 | 839 | M | iBRAF* | 25 | on | prostate cancer |
| 44 | 749 | M | iBRAF* | 16 | on | prostate cancer |
| 45 | 898 | M | iBRAF* | 24 | on | prostate cancer |
| 46 | 899 | M | iBRAF* | 27 | on | no obvious tumors |
| 47 | 900 | M | iBRAF* | 23 | on | no obvious tumors |
| 48 | 913 | M | iBRAF* | 20 | on | prostate cancer |
| 49 | 905 | M | iBRAF* | 32 | on | prostate cancer |
| 50 | 908 | M | iBRAF* | 32 | on | prostate cancer |
| 51 | 920 | M | iBRAF* | 25 | on | no obvious tumors |
| 52 | 914 | M | iBRAF* | 29 | on | prostate cancer |
| 53 | 910 | M | iBRAF* | 30 | on | lymphoma |

**B. Line 13**

| Number | | Sex | Genotype | Age of death(weeks) | Doxy | Pheotypes |
|---|---|---|---|---|---|---|
| 1 | 226 | M | iBRAF* | 13 | on | no obvious tumors |
| 2 | 248 | M | iBRAF* | 11 | on | no obvious tumors |
| 3 | 294 | M | iBRAF* | 5 | on | no obvious tumors |
| 4 | 346 | M | iBRAF* | 17 | on | prostate cancer |
| 5 | 347 | M | iBRAF* | 38 | on | melanoma |
| 6 | 350 | M | iBRAF* | 22 | on | prostate cancer |
| 7 | 419 | M | iBRAF* | 28 | on | melanoma |
| 8 | 423 | M | iBRAF* | 4 | on | no obvious tumors |
| 9 | 450 | M | iBRAF* | 30 | on | prostate cancer |
| 10 | 539 | M | iBRAF* | 36 | on | sarcoma |

[a] Tet-Braf$^{E600}$+, Tyr-rtTA+, Ink4a/Arf -/-

[b] Tet-Braf$^{E600}$+, Tyr-rtTA-, Ink4a/Arf -/-

[c] Age of the mouse that had been sacrificed for the detailed histological examinations due to the visible tumor formation

## Conclusion

Taking advantage of our novel genetically-engineered mouse (GEM) model of invasive prostate adenocarcinoma, we expressed an activating mutation of $BRAF^{V600E}$ in an inducible manner under the control of a unique androgen-insensitive promoter. For the first year, we attempted to address the second proposed specific aim first; *to assess the requirement for continuous BRAF*-ERK activation in maintenance of established invasive lesions and in progression to androgen-independent state*. In spite of several difficulties, such as high mortality of tumor-bearing iBRAF transgenic mice, applying an alternative tissue recombination system, we accomplished two main findings. First, **constitutive activation of BRAF/ERK/MEK signaling is NOT required for iBRAF* tumor maintenance**; While MAPK activation alone can initiate prostate tumorigenesis, continued mutant BRAF expression or downstream MAPK activation is not required for maintenance of established PCA in iBRAF* model. Second, **constitutive activation of BRAF/ERK/MEK signaling is NOT sufficient to drive active AI growth under an androgen-limited state**; While MAPK activation may be permissive for survival post castration, BRAF driven MAPK activation is not sufficient to drive active AI growth under an androgen-limited state. These findings suggest several future directions related to AI prostate cancer research. First, we need to identify other signal transduction pathways related to development of AI tumors in cooperation with MAPK pathway, and then combinational intervention strategy for the identified pathways should be considered as a future therapy in particular for the treatment of advanced AI tumor. Finally, the presence of residual p63+ cancer cells after castration suggested possible role(s) of putative stem cell compartments, such as Sca-1 + cells, in the cell-of-origin of androgen independent prostate cancer. Further research related to the cell-of-origin of p63+ cells after castration will lead us to address the first proposed specific aim; *to characterize the Sca-1+ cells in iBRAF* prostate epithelium and tumor.*